A Cantilevered DeltaXY Positioning Mechanism Enabling Rackable Digital Fabrication Form Factors

Ilan E Moyer
Department of Mechanical Engineering
Massachusetts Institute of Technology
Cambridge, Massachusetts, USA
imoyer@mit.edu

Leo McElroy
Independent Researcher
Cambridge, Massachusetts, USA
leomcelroy@gmail.com

Quentin Bolsée
Center for Bits and Atoms
Massachusetts Institute of Technology
Cambridge, Massachusetts, USA
quentinbolsee@hotmail.com

Joshua Rivera Camacho
Department of Mechanical Engineering
Massachusetts Institute of Technology
Cambridge, Massachusetts, USA
joshua47@mit.edu

Jennifer Jacobs
Media Arts and Technology
University of California Santa Barbara
Santa Barbara, California, USA
jmjacobs@ucsb.edu

Maria Yang
Department of Mechanical Engineering
Massachusetts Institute of Technology
Cambridge, Massachusetts, USA
mcyang@mit.edu

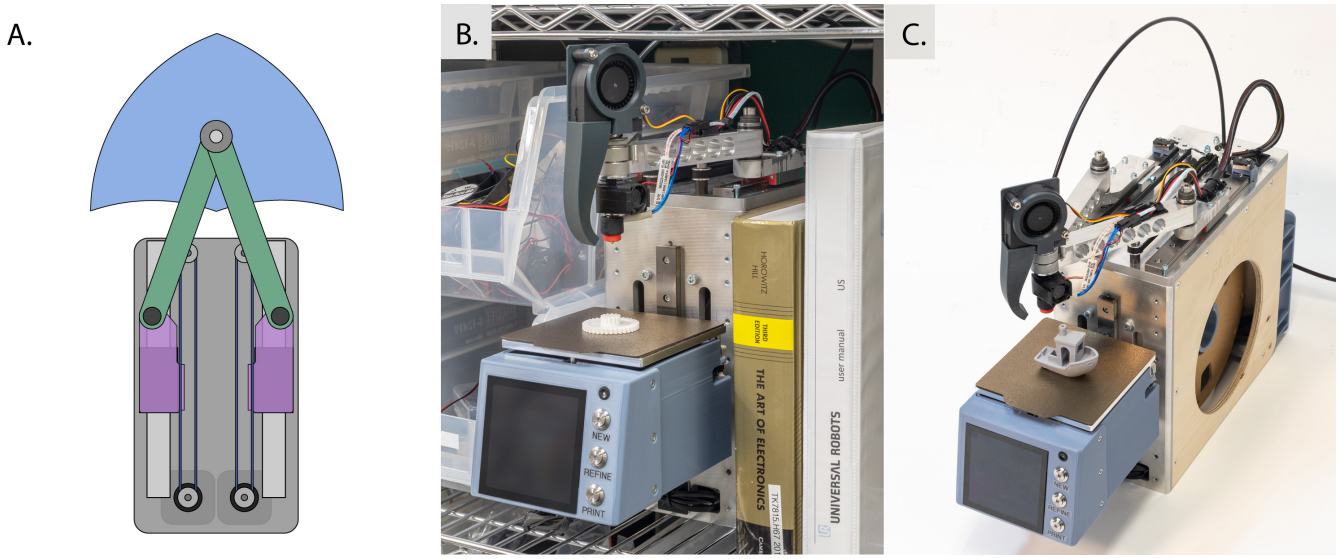

Figure 1: A) Cantilevered DeltaXY is a parallel kinematic positioning mechanism that exhibits high lateral spatial efficiency (LSE). B) This enables novel digital fabrication machine form factors designed for space-constrained settings including shelves and high-density rack systems, rather than the desktop, suggesting new application domains. C) We explore DeltaXY through the design of Fab Unit, a bookshelf 3D printer with best-in-class LSE compared to commercially available machines.

Abstract

Desktop digital fabrication presumes form-factors designed for workbenches, limiting suitability for other spaces and workflows. We propose a class of physically narrow and deep "rackable" digital fabrication machines that offers opportunities for new applications and interactions. Flexible and inconspicuous placement supports ubiquitous fabrication, including site- and context-specific tools. Personal factories could be enabled by shelf-optimized rackable digital fabrication technologies that improve organization and functionality for collections of machines. These explorations necessitate new positioning mechanisms and machine architectures. We contribute the Cantilevered DeltaXY mechanism that enables rackable digital fabrication form factors with high lateral spatial efficiencies (LSE). We develop first-order design tools to aid the implementation of DeltaXY machines. We demonstrate DeltaXY by creating Fab Unit, a "bookshelf 3D printer" with an LSE significantly higher than similar commercial desktop machines. Together, DeltaXY and Fab Unit open the design space of rackable digital fabrication for future HCI fabrication research.

CHI '26, Barcelona, Spain

ACM ISBN 979-8-4007-2278-3/26/04
https://doi.org/10.1145/3772318.3791468

CCS Concepts

• **Human-centered computing → Human computer interaction (HCI)**; • **Applied computing → Computer-aided manufacturing**; • **Hardware → Electro-mechanical devices**; *Printers.*

Keywords

rackable digital fabrication, 3D printing, DeltaXY, hardware prototyping, ubiquitous fabrication

ACM Reference Format:

Ilan E Moyer, Leo McElroy, Quentin Bolsée, Joshua Rivera Camacho, Jennifer Jacobs, and Maria Yang. 2026. A Cantilevered DeltaXY Positioning Mechanism Enabling Rackable Digital Fabrication Form Factors. In *Proceedings of the 2026 CHI Conference on Human Factors in Computing Systems (CHI '26), April 13–17, 2026, Barcelona, Spain.* ACM, New York, NY, USA, 26 pages. https://doi.org/10.1145/3772318.3791468

1 Introduction

Over the past twenty years, numerical control, invented in the 1950s as an industrial technology, has leapt from the factory floor to the desktop. Forbes reports sales of desktop 3D printers approached 1M units in Q4 2023 [56], indicating a meaningful shift towards hobbyist and professional end-users rather than industrial machine operators. Today, "desktop" digital fabrication represents *both* a physical form factor optimized for cost and compactness on a desk or workbench, *and* a class of user. This parallels the early trajectory of personal computing, where the centralized mainframes of the 1960s turned into the personal, desktop computers of the 1970s and 1980s [15]. The proliferation of low-cost computers brought about new applications that necessitated alternative forms, including the laptop and smartphone for on-the-go computing, and the rack server (and later blade server) for dense, scalable packing of modular computing equipment.

Just as widespread computing adopted new physical forms to take advantage of emerging applications, we argue that alternative form factors for sub-industrial scale digital fabrication equipment — beyond those designed for the desktop — could enable new domains of use and interaction. Digital fabrication technologies optimized for *shelving* are currently unexplored and offer interaction and workflow advantages distinct from those of desktop machines. Shelving and shelf-like spaces represent a valuable class of storage in residential, office, and workshop settings, and could unlock more convenient, diverse, and ambient placement of digital fabrication tools. Shelf-optimized digital fabrication tools may enable print farms that occupy less space: like servers in a rack, the packing density of these printers directly impacts physical space requirements and/or capacity, thereby suggesting new contexts and applications that could include rapid at-home parallelized production of assemblies, or mobile fabrication carts (e.g. [35]) that are higher density to simultaneously engage many students in digital fabrication classroom activities. As accessible design tools become increasingly powerful, we anticipate a growing interest in fabrication pipelines that cascade multiple processes to produce objects that cannot be created with a single-purpose machine. "Personal factories" could be realized in a modular, space-efficient way through rack-mounted fabrication machines connected by a workpiece-transit system. This vision is a natural extension of prior work on multi-process fabrication using tool-changing within a single machine [72]. These directions have implications for how users interact with digital fabrication and how it impacts them.

In order for HCI researchers to investigate the interaction possibilities of shelf-optimized *rackable digital fabrication* tools, actionable platforms are needed on which to prototype and test new technologies. Prior work explores the design space for desktop [37, 72] and mobile [8, 45, 54] machine architectures, but approaches for space-constrained digital fabrication machines are currently lacking. In this paper, we investigate how digital fabrication tools can be architected to take advantage of the unique characteristics of living on a shelf, where frontage is at a premium, while depth is free within limits. This suggests a design optimization for *lateral spatial efficiency* (LSE), which we define as the ratio of working area width to machine width. A survey of commercially available desktop fused-filament fabrication (FFF) 3D printers reveals LSEs ranging between 29% and 73%, which tend to increase with working area width due to a fixed overhead of their underlying positioning mechanisms. We introduce the *Cantilevered DeltaXY* (DeltaXY) 2D positioning mechanism, that can achieve an LSE approaching (and in some cases exceeding) 100%, at the expense of depth-wise efficiency. DeltaXY builds on a known parallel kinematic mechanism (PKM) topology, and applies it in a unique way that projects the toolhead in front of the machine while allowing it to reach laterally beyond the extents of its guide rails. Beyond improved LSE, these attributes have potential implications for allowing cooperative operation of adjacent machines in partially or fully shared workspaces, and for configurations that go beyond the shelf. To practically explore the DeltaXY mechanism, we designed and built Fab Unit, a bookshelf FFF 3D printer with a build area of approximately 120x120mm that occupies a shelf width of 127mm, leading to an exceptionally high LSE of 94%. [1]

Our work aligns with and extends established challenges in HCI digital fabrication research. Foremost, rackable fabrication offers a new dimension for enabling ubiquitous personal fabrication– a long-running theme in HCI research [5, 16]. Thus far, personal fabrication has primarily been explored through low-effort computer-based interfaces [62]. Yet studies of actual fabrication practice suggest that minimizing the physical effort to access a tool through at-hand placement can improve workflows and process satisfaction [3, 29]. We see opportunities to create new design contexts for casual [24], immediate [25], and spontaneous [66] digital fabrication use through flexible form factors that support the diffusion of digital fabrication into our living and working spaces. We discuss how architectures enabled by the Delta XY mechanism could support interactions that are not computer-centric, but rather occur at the tool in a manner more similar to today's household appliances. We also suggest opportunities for specialized fabrication tools tailored to context-of-use and location.

We contribute:

- The Cantilevered DeltaXY positioning mechanism as an enabling contribution for HCI researchers to investigate the design space of rackable digital fabrication, supported by a

[1] The metric of LSE becomes nuanced when a mechanism is not constrained by a concrete machine envelope, as addressed in Section 9.2.

set of first-order analyses, guidelines, and a browser-based design tool to aid researchers in developing new DeltaXY-based digital fabrication machines.
- Fab Unit as a working example of a DeltaXY-based digital fabrication tool optimized for shelf placement, including a discussion of encountered design considerations and a qualitative demonstration of its function.

To support future research and development efforts in rackable digital fabrication, we make publicly available the Cantilevered DeltaXY mechanism, Fab Unit design data, software design tools, and Klipper motion control kinematics, under non-commercial open-source licenses[2].

We begin by presenting an overview of related work, including a survey of the lateral spatial efficiency of commercially-available 3D printers. We continue with an overview of the DeltaXY mechanism, followed by a detailed examination of Fab Unit as a realized example. We discuss early visions for rackable digital fabrication and the potential of the DeltaXY mechanism, based on our experiences so far. We follow this with a "guidebook" to aid researchers in extending DeltaXY to new machine designs, and conclude with a discussion of limitations.

2 Related Work

This paper proposes the Cantilevered DeltaXY positioning mechanism as an enabler of rackable digital fabrication machine form factors, providing concrete design knowledge that allows researchers to explore sub-industrial digital fabrication tools that are more readily at-hand, more space-efficient, and that one day might collaborate in automated multi-process workflows. In this section we start by reviewing work that demonstrates a rich history of machine building within HCI that has supported the exploration of novel fabrication interactions, workflows and processes, including form-factors beyond desktop digital fabrication. We provide results of a quantitative survey of the lateral spatial efficiencies (LSEs) of commercially available 3D printers, situating the DeltaXY-enabled Fab Unit bookshelf 3D printer along an important metric for rackable digital fabrication tools. We then review work related to the DeltaXY mechanism, drawn largely from the field of parallel kinematic mechanisms (PKMs) [36], and conclude with alternative approaches to achieving high LSE.

2.1 Machine Building as an HCI Research Activity

Research examining new ways of interacting with digital fabrication tools often requires the construction of novel fabrication hardware. Within the sub-field of interactive fabrication [73], custom hardware enables direct physical engagement with a process. Tian et al. built a lathe with haptic handwheels to examine high-feedback "lucid fabrication" [67]. Rivers et al. constructed a handheld CNC router with a unique positioning mechanism to explore collaborative approaches to hybrid fabrication [54]. In the same vein, Zoran and Paradiso created an actuated dremel tool for hybrid carving [77]. Moyer et al. reimagined the pottery wheel as a clay 3D printer to explore craft-centric CNC interactions [39].

[2]http://www.deltaxy.org

Machine building has supported explorations into the interaction affordances of *automated* fabrication form-factors that go beyond the desktop. Peek et al. examined the implications of portable 3D printing through the construction of PopFab [45], and Campos Zamora et al. explored the design space of environmental-scale fabrication with an automated mobile 3D printer [8]. HCI digital fabrication research has also involved the modification of existing machine hardware. For example, Rivera and Hudson explored opportunities for multi-structural 3D printing by modifing a 3D printer to produce electrospun textiles [53], and He and Adar examined accessible punch-needle embroidery through a modified pen plotter [23].

Researchers have acknowledged the value of toolkits to scaffold the physical construction of new machines. Peek et al.'s Cardboard Construction Kit [44] allows playful experimentation with machine building through low-fidelity prototyping. Vasquez et al. provide an open-source machine platform for interchangeable toolheads [72], enabling the exploration of new multi-process fabrication approaches. Fossdal et al. developed a machine-building technique and set of modular designs that can be realized using accessible fabrication tools [13]. However, HCI research supporting the practice of machine building has primarily focused on control systems, including modular and distributed approaches [38, 46, 51, 52], live control from creative environments [12, 64], live parameter tuning [65], and workflow development [14, 69, 70], rather than generalizable physical construction approaches. We seek to address this knowledge gap by providing design support for alternative CNC mechanisms.

The above body of work demonstrates how machine building unlocks areas of inquiry for digital fabrication HCI research, which is our motivating goal. We are unique in that we provide an enabling framework for exploring the interaction and workflow possibilities of a new class of space-constrained, rackable machine architectures. In contrast, prior work has either provided frameworks for building existing architectures (e.g. [13, 44]), or focused on unique affordances of specific machines [72]. To our knowledge, approaches to space-constrained digital fabrication remains an unexplored domain.

2.2 Lateral Spatial Efficiency, and Limitations of Commercial Mechanisms for Rackable Fabrication

Many digital fabrication processes depend on precisely positioning a toolhead (e.g. a 3D printing extrusion nozzle, machining spindle, laser beam, etc.) in 3+ dimensions relative to a workpiece or machine bed. Figure 2 A-D provides a graphical overview of common positioning mechanisms employed for this task. Almost universally, commercial machine architectures place motors and mechanism elements at the periphery of the work area, fundamentally limiting their spatial efficiency by confining the travel of the toolhead (see Fig. 3). In particular, the *lateral* space requirements of digital fabrication machines directly impact where and how densely they can be placed in constrained environments such as shelves. We assess machine architecture implementations for *rackability* by defining the metric of *lateral spatial efficiency (LSE)* as the ratio of workspace width to overall machine width (i.e. $LSE = \frac{W}{W_M}$, see

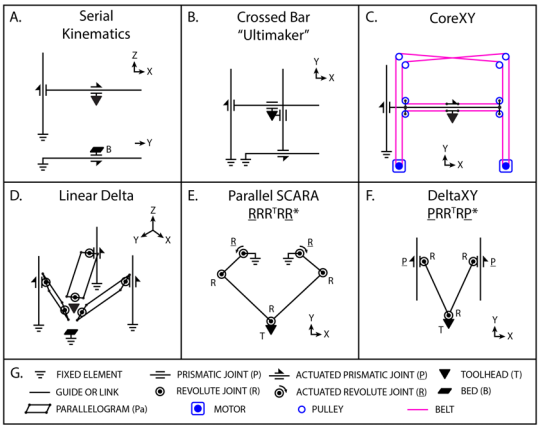

Figure 2: Common 3D printing kinematics (A-D), alongside DeltaXY (F) and its cousin the parallel SCARA (E). *Topological notation expands on [34, 36] to include positions of bed and toolhead.

Fig. 3). When used retrospectively on existing commercial machine designs, the lateral dimension is measured across whichever machine face the manufacturer has designed as the front — often cued by workspace access or user interface location — corresponding to how the machine would naturally be placed for operation on a shelf.

To provide an understanding of typical LSEs for commercially available (or recently available) digital fabrication machines, we benchmarked 19 FFF 3D printers based on manufacturer-provided specifications[3] (Figure 4). LSEs range from 29% to 73%, and generally improve with build area width due to a relatively fixed overhead of the positioning mechanism. There was no kinematic architecture that universally did better or worst, suggesting that much depends on specific implementation. We chose to focus on 3D printing for this survey because it is a dominant form of desktop digital fabrication, employs a variety of positioning mechanisms, and has

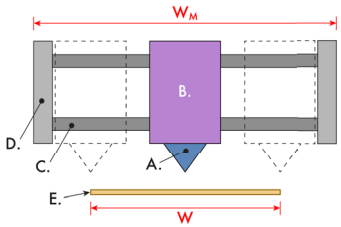

Figure 3: A canonical positioning stage: a toolhead (A) is attached to a carriage (B), that runs on guides (C) supported by machine structure (D). Motion of the toolhead is limited to width (W) over a workspace (E), while the machine occupies a width of (Wm).

[3]Positron provides machine dimensions in a folded state. We referred to their open-source CAD to determine lateral footprint when in its operating configuration.

Figure 4: Lateral spatial efficiencies of commercially available 3D printers in comparison with Fab Unit, defined as the ratio of build area width to overall machine width. For Fab Unit we additionally provide a bounding *minimum LSE (MLSE)* metric (see Sec. 2.4)

.

been the subject of extensive research and commercial development in recent years.

2.3 Work Related to the DeltaXY Kinematics

Parallel kinematic mechanisms (PKMs) utilize multiple structural loops that pass through at least two independent kinematic chains, and can be advantageous in terms of accuracy, stiffness, and dynamic performance [42]. In contrast, serial kinematics (Fig. 2A) stack axes on top of each other, aggregating errors and mechanical compliances, and limiting acceleration. The Cantilevered DeltaXY mechanism described in this paper belongs to a family of 2D PKMs that consist of two actuated Prismatic (i.e. linear) joints coupled to a toolhead through three Revolute joints (Fig. 2F) — subsequently referred to as PRRRP kinematics using the notation of McCloy [34] and Merlet [36]. Closely related is the parallel selective compliance articulated robot arm (SCARA) [75], with a purely revolute kinematic chain of RRRRR (Fig. 2E). The PRRRP kinematics were described as early as 1990 by McCloy [34], and have been commercially deployed in machining centers [2, 22], where the mechanism is oriented vertically to actuate a horizontal machining spindle, and offsets the spindle from the central revolute joint. To our knowledge, these kinematics were first experimented with for 3D printing by PavloG on the RepRap forum in 2016, who oriented the mechanism horizontally to actuate an extruder placed concentrically with the central revolute joint [43]. They introduced the term "DeltaXY" to describe these kinematics; for brevity, we take the liberty of referring to Cantilevered DeltaXY simply as DeltaXY throughout this paper.

A characteristic of the PRRRP kinematics is that the toolhead rotates with one of the linkage arms. This requires that the toolhead axis be orthogonal to the plane of motion of the linkage. Liu et al.

introduced a kinematically equivalent vertically-oriented 2D positioning system where four-bar parallelogram structures maintain the orientation of a central mounting plate [31]. They applied it to the XZ plane of a machine tool, where the spindle axis is vertically oriented. In the open-source 3D printing community, this vertically-oriented kinematic configuration was explored under the name *Deltesian* [55]. Melena et al. adapted Liu's kinematics to an infinite-belt 3D printer, where the positioning mechanism lies in a canted plane relative to the print bed [10]. Son et al. developed a hybrid 5-axis milling machine (the MIT-SS-1) that utilizes a 3-PRR PKM operating in the vertical plane to realize two translational and one rotational degrees of freedom [61]. Here, Lui's parallelogram structure has been replaced with a third actuated link to control in-plane rotation of the toolhead.

In all PRRRP examples known to us, the linkage arms operate in a plane that passes through the outer prismatic bearings, which limits LSE by requiring the mechanism to operate within the lateral bounds of the machine to avoid colliding with the bearing rails. Additionally, only PavloG's implementation is oriented horizontally, but is not structured to extend the tool-head past the front edge of the machine. The 3-PRR mechanism of Son et al.'s MIT-SS-1 operates in a vertical plane that is offset from its prismatic bearings for manufacturing reasons, but is not designed to operate near the machine extents, and achieves an LSE of up to 33%. **Our enabling mechanism contributions are the complementary ideas of placing the linkage arms on a plane above the prismatic bearings and operating the toolhead in front of the machine's static structure. These innovations permit Cantilevered DeltaXY to achieve an LSE that exceeds unity, and provide the ability for multiple machines to share a common workspace.**

2.4 Alternative Approaches to Cantilevered Motion and High LSE

Digital fabrication machines such as the Bantam Tools Nextdraw 8511 [68] (formerly "Axidraw") pen plotter cantilever the toolhead in front of the machine base, providing flexibility to locally operate on large workpieces, and excellent access to the workspace. However, they are not designed for rackability. For example, the Nextdraw 8511 has an LSE of 55%, equivalent to the Bambu A1 Mini [26] 3D printer. Cincinnati Milacron's High Speed Machining Center (HSMC) — an industrial horizontal milling machine — projects its spindle horizontally in front of the machine to enable *duplexed* operation with an opposing machine on a shared workspace (see [60, pp. 31-44]). DeltaXY combines the benefits of a cantilevered toolhead with a high LSE, enabling shared workspaces with *adjacent* machines.

Researchers and industry have developed machines that can access work areas larger than themselves. Rivers et al. developed a handheld CNC router to work on full sheets of plywood [54]. Campos Zamora et al. created a mobile 3D printer that operates on flooring [8]. While these approaches achieve high LSE, they do so by enabling very large working areas, making this approach unsuitable for shelf-based fabrication. For example, Shaper Origin [57] — the commercial offshoot of Rivers et al.'s research — has a fixed width of 339mm and an automated workspace of only 12mm in diameter, resulting in an LSE that starts at 3.5% while occupying significant shelf space. Arcdroid [9] and 3D Potter [48] have developed robot arms (based on Makino's SCARA serial mechanism [32]) that perform plasma cutting and clay 3D printing, respectively, on work areas much larger than the machine. While these mechanisms could conceivably be scaled down to operate on a shelf, they have "elbows" that may extend outside the width of the base and collide with adjacent objects. In contrast, DeltaXY's toolhead always leads the mechanism when outside the lateral bounds of the machine, minimizing the potential for interference. The Delta Keops [7] is a top-mounted 3-axis PKM capable of reaching past its lateral extents, and is designed for high-speed industrial pick-and-place and assembly operations within a shallow cylindrical workspace. This mechanism requires significant height to operate, limiting its suitability for shelf-based applications.

The metric of LSE becomes more nuanced for machine architectures that enable the work bed or toolhead to operate outside the static bounds of the machine. "Bed slingers" such as the Prusa Mk4s [4] actuate a low work bed along the Y axis outside the extents of the machine, and require additional front or rear clearance to avoid colliding with adjacent objects. This direction of travel is rarely designed to be parallel to the front of the machine. However, if it were, then the machine width should account for the bounding travel of the bed, because there are no practical shelf-born configurations that mitigate the risk of collision. For mechanisms where *toolhead* motion may exceed the lateral bounds of the static machine base, as is the case with the Cantilevered DeltaXY mechanism, the LSE ratio of workspace to base width can still be meaningful if opportunities for interference are limited and controllable. We suggest an additional metric of *minimum LSE (MLSE)* using toolhead travel bounds rather than fixed machine width as its divisor, as it may be meaningful in certain situations. We discuss this edge case of the LSE metric in Section 9.2 once additional context has been established.

3 The Cantilevered DeltaXY Mechanism

We developed the Cantilevered DeltaXY mechanism to enable rackable digital fabrication machine architectures that are optimized for compact placement on shelving. Such a machine should:

- efficiently occupy lateral shelf space. We define the key metric of *lateral spatial efficiency (LSE)* as the ratio between a machine's working width and its chassis width.
- minimally interfere with adjacent machines or objects, allowing machines to be tightly placed.

Cantilevered DeltaXY (DeltaXY) is a multi-purpose 2D positioning mechanism that achieves high lateral spatial efficiency (LSE) by projecting a toolhead in front of a narrow, deep fixed base, and reaching up to or even past the lateral edges of the machine. In contrast, commercial desktop digital fabrication machines almost universally operate within a fixed chassis that limits LSE, and assume form factors proportionally more akin to a toaster oven than a book.

In this section we share a reference implementation for DeltaXY that embodies our enabling ideas and is readily adaptable and manufacturable, followed by an overview of DeltaXY's kinematics and performance considerations. In Sections 7 and 8 we develop design

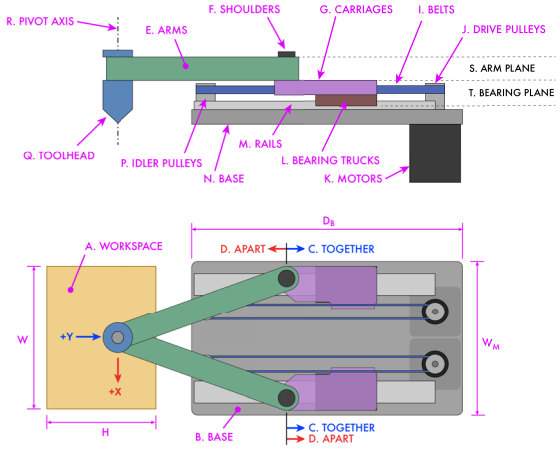

Figure 5: DeltaXY Reference Implementation

heuristics, first-order performance scaling laws, and a browser-based design tool, to empower HCI researchers to further explore the possibilities afforded by DeltaXY.

3.1 Reference Design

Figure 5 illustrates a reference design introducing the DeltaXY mechanism that we incorporate into the Fab Unit bookshelf 3D printer in Section 4. A compact toolhead (5Q) (e.g. a 3D printing nozzle, small spindle, laser diode, etc...) is cantilevered over the front edge of the machine at the end of two arms (5E), and fixed to one of the arms concentrically with a pivot axis joining the arms (5R). Each arm is supported at its other end by a revolute shoulder joint (5F), permitting free rotation but resisting radial and pitch-moment loads. Each shoulder is mounted to a carriage block (5G) affixed to linear bearing trucks (5L) and independently actuated along parallel guide rails (5M) by stepper motor-driven belt drives (5I, J, K, P). The carriages project the shoulders ahead of the trucks, providing a useful degree of freedom when optimizing

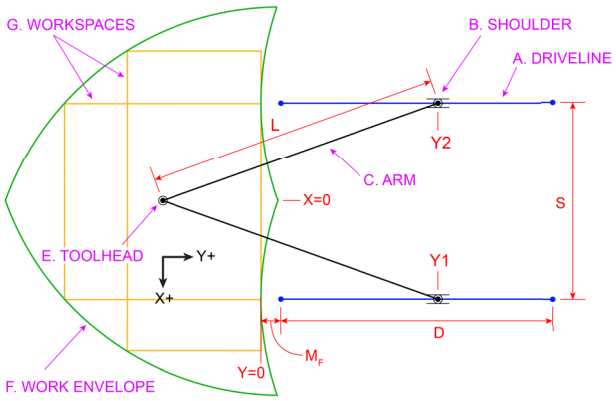

Figure 6: DeltaXY Linkage Parameters

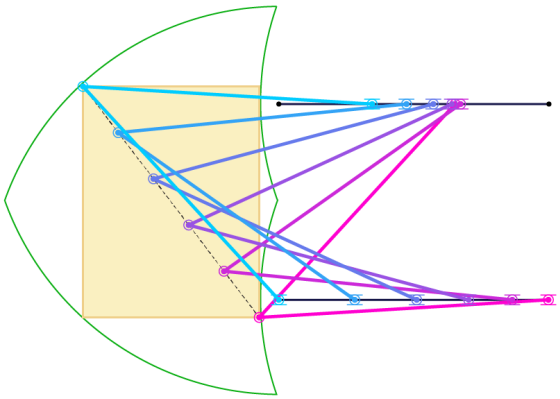

Figure 7: DeltaXY Motion

performance. Importantly, the arms rotate in a plane (5S) that is above that of the carriages and bearings (5T), permitting free rotation outside the bounds of the bearing rails. This distinguishes our design from prior work, and enables a far greater range of lateral toolhead motion. When both carriages move in the same direction (5C), the toolhead moves purely in the Y direction. When the carriages move in opposite directions (5D), the toolhead sweeps an arc primarily in the X direction. In this way, the Cantilevered DeltaXY mechanism is able to access a workspace that lives outside the fixed bounds of the machine, and whose width may exceed that of the machine base. Besides implications for LSE and form-factor, this arrangement allows a common workspace to be accessed by multiple adjacent machines. By combining DeltaXY with an independent Z axis, three-axis digital fabrication machines can be realized, as demonstrated by Fab Unit in Section 4. The reference design is organized around a base plate (5N) to which the guide rails and drivetrain are mounted, providing a simple structure that is easily incorporated into specific machines, readily adapted for varied configurations, and can be fabricated from a wide range of materials using commodity processes such as laser cutting, waterjet cutting, or CNC milling. Additionally, Son et al. demonstrate that mounting bearing rails to a common surface minimizes coplanarity errors, thereby reducing mechanism overconstraint [61].

3.2 DeltaXY Kinematics

The DeltaXY PRRRP kinematics are shown schematically in Figure 6, and represent the skeleton of the reference design of Figure 5. They consist of two arm links (6C) that meet at a revolute joint R nominally concentric with the toolhead (6E). The opposite ends of each arm are constrained by a revolute shoulder joint R coincident with an actuated prismatic joint P (6B), such that they are constrained along two parallel drivelines (6A) while being free to rotate. Figure 7 illustrates the travel of the toolhead, arms, and shoulders while tracing a diagonal of the workspace. When the toolhead is outside the region between the drivelines, it always leads the arms.

The DeltaXY mechanism is fully defined by just three parameters: link length L, driveline length D, and driveline separation S. A shield-shaped maximal toolhead *work envelope (WE)*(6F) is defined

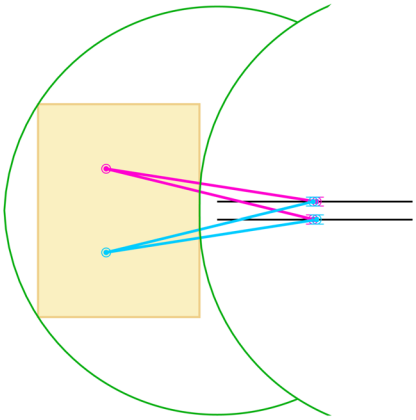

Figure 8: High $\frac{L}{S}$ yields poor resolution and stiffness.

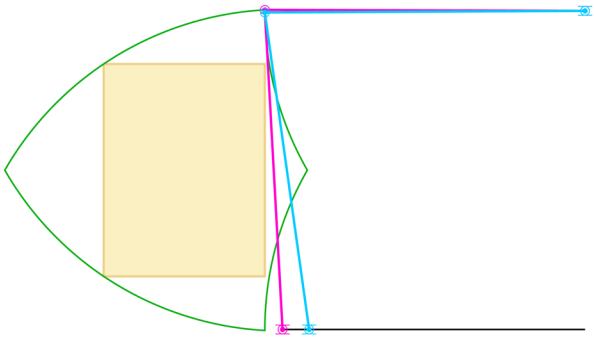

Figure 9: Low $\frac{L}{S}$ yields poor acceleration at workspace edges.

by the region between four arcs, each centered at one endpoint of the drivelines with a radius L. The irregular shape of the WE can make it difficult to communicate the work capacity of a machine, and rectangular *workspaces* of many proportions can be inscribed within the WE (3.2G). A *front margin* M_F separates the start of the drivelines from the base of the WE, and can be used as an alternative parameter to drive linkage design.

3.3 Performance Considerations

The DeltaXY mechanism is *non-linear*, and the relationship between actuator and toolhead motion varies with X-axis position. This has implications for performance characteristics such as positioning resolution, rigidity, and dynamic performance. We provide an overview here, and greater depth in Sec. 7.

3.3.1 Positioning Resolution. Positioning resolution bears on the smoothness, minimum feature size, and accuracy of a digital fabrication machine's work. DeltaXY has a constant Y-axis toolhead positioning resolution that is equal to that of the actuators. In the X direction, actuator resolution is amplified or attenuated at the toolhead by a gain factor that reaches a maximum at $X = 0$, and approximately scales with $\frac{L}{S}$. Figure 8 provides an illustrative example when $\frac{L}{S} \rightarrow \infty$ and the mechanism approaches a "Type 3" singularity [20], which is when the mechanism collapses because both arms become co-linear; a small motion of either actuator results in a very large motion of the toolhead. In the reference design of Fig. 5, actuator motion is amplified by a factor of 1.4 in the X direction. To counteract this, machine designers may increase actuator resolution, for example through alternative stepper motors (e.g. $400\frac{steps}{rev}$ vs $200\frac{steps}{rev}$) or smaller timing belt pulleys, which may affect dynamic performance. For more details see Section 7.5.

3.3.2 Rigidity. The rigidity or stiffness of a positioning mechanism relates toolhead forces to resulting deflection, and is the inverse of compliance. This metric influences how accurately a toolhead can be positioned under loads caused by interaction with a workpiece or toolhead acceleration, and whether the tool vibrates excessively, affecting surface finish. Just as the DeltaXY linkage may amplify actuator motion at the toolhead, in-plane forces applied to the toolhead may amplify at the actuator (as intuited from Fig. 8). The result is a *lateral compliance gain* from the actuator to the toolhead that is highest at $X = 0$, and approximately scales with $\left(\frac{L}{S}\right)^2$. In the reference design of Fig. 5, actuator compliance is amplified by a factor of 3.9. Major sources of actuator compliance are timing belt stretch and the magnetic stiffness of the stepper motor. To counteract these, designers may use higher-resolution stepper motors, smaller timing belt pulleys, stiffer belts, or reduce belt length. DeltaXY places the toolhead at the end of cantilevered arms, which is disadvantageous for Z-axis stiffness. This is addressed through the design of the arms, shoulders, carriages, and linear bearings to provide adequate stiffness. For more details see Section 7.6.

3.3.3 Dynamic Performance. The ability of a digital fabrication machine to accelerate its toolhead impacts the speed of processes that are inertia-limited, such as FFF 3D printing [18]. DeltaXY accelerates the slowest at the lateral edges of the workspace. Figure 9 provides an illustrative example when $S \rightarrow L$ and the mechanism approaches a "Type 1" singularity [20], which is a configuration where large motions of the actuator generate very small motions of the toolhead. This benefits positioning resolution and stiffness, but significantly degrades dynamic performance because the actuator must accelerate its own mass quickly for minimal acceleration of the toolhead. The use of higher actuator reductions, such as with small timing belt pulleys, exacerbate this issue. We estimate that for the reference design of Fig. 5 as embodied by Fab Unit (Sec. 4), dynamic performance varies by about 20% over the workspace, but remains equivalent to commercial desktop 3D printers. For more details see Section 7.8.

4 Fab Unit: a DeltaXY Bookshelf 3D Printer

Fab Unit is a self-contained *bookshelf 3D printer* that assumes the form factor of a thick book or catalog to fit compactly on a shelf alongside books or other objects (Fig. 1B & 1C), enabled

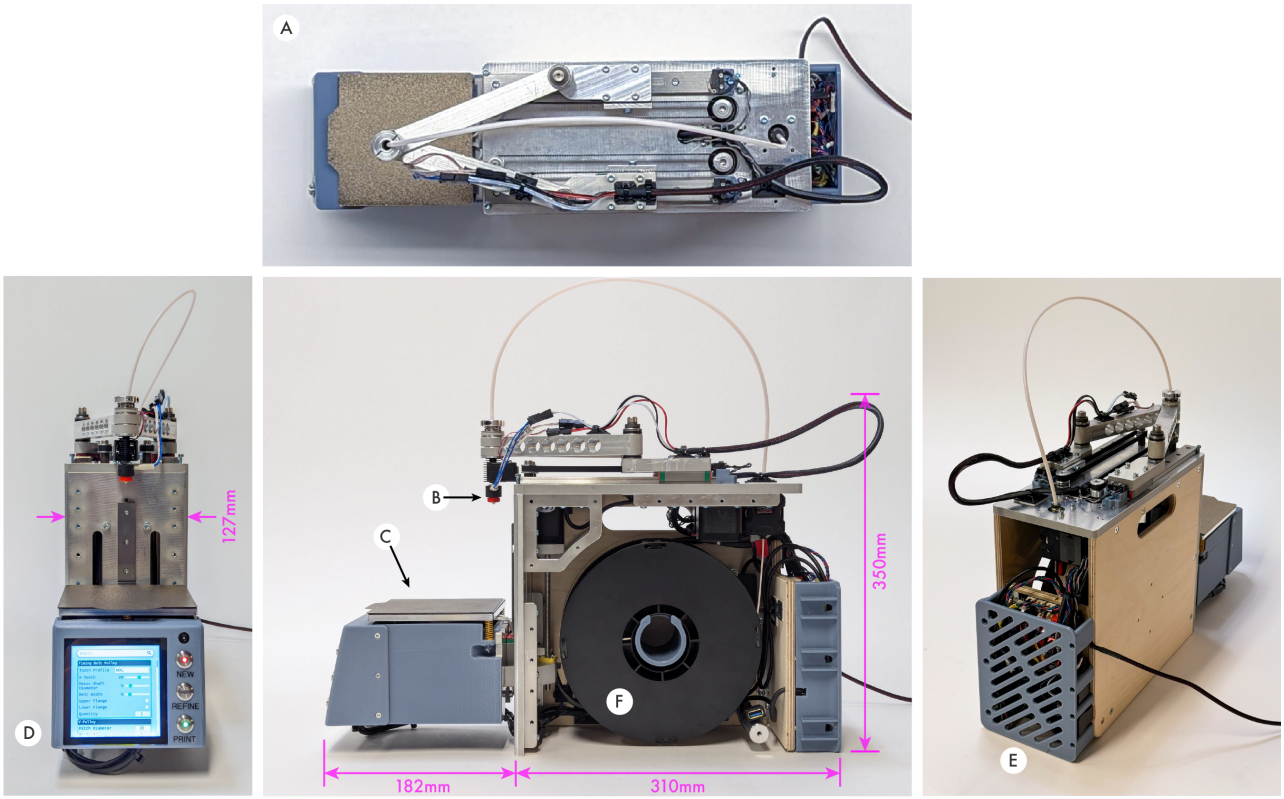

Figure 10: The Fab Unit Bookshelf 3D printer. A) DeltaXY positioning system, B) FFF printhead, C) Z axis with heated build platform, D) Display to support onboard user interfaces, E) Motion controller, F) Filament spool

by the DeltaXY mechanism. It has a build area of approximately 120x120mm, yet occupies 127mm of shelf width, leading to an exceptionally high LSE of 94%. We built Fab Unit to practically explore the form factor opportunities afforded by DeltaXY, and as a testbed for future explorations into implications of form factor and placement on digital fabrication use and the interface approaches that might support this shift. Fab Unit's design files, bill of materials, and Klipper kinematics extensions are available online under non-commercial open-source licenses[4].

Figure 10 shows Fab Unit's overall architecture, which includes: the DeltaXY positioning system (10A), an FFF printhead (10B), a Z axis with heated build plate (10C), a touch display for interface explorations (10D), a motion controller with onboard Linux computer (10E), and a nested filament spool (10F). Fab Unit has an overall depth of 492mm (19.4") and a fixed base depth of 310mm (12.2"), allowing to it securely plant on standard 12"-deep shelving with the build platform overhanging. It stands 350mm tall (not including the Bowden filament guide tube). In the following sub-sections we describe key architectural decisions and design details, discuss Fab Unit's workspace with implications for the metric of LSE, share print results as proof-through-demonstration of DeltaXY's performance for FFF 3D printing, and discuss the calibration steps required to achieve these results.

[4]http://www.deltaxy.org

4.1 Machine Design

When establishing Fab Unit's overall architecture, we sought to treat the DeltaXY stage as a modular design element. This led us to design Fab Unit around a top aluminum structural plate containing DeltaXY, which we extended rearward to accommodate a filament extrusion motor. Aluminum ribs connect DeltaXY to a vertical aluminum plate that supports an independent Z axis assembly, consisting of a stepper motor with integrated leadscrew, a linear bearing rail and truck, and a 3D-printed carriage supporting an off-the-shelf heated build plate. We placed a filament spool in the void formed by the top and front plates, with the goal of making Fab Unit entirely self-contained. The remainder of the chassis is formed by plywood panels fastened to the aluminum ribs. An electronics package containing stepper drivers and a Linux CPU live inside a vented 3D printed housing at the rear of the machine. Lifting handles are provided on the sides. We chose to use a Bowden-tube configuration for the 3D printhead, which separates the heated extrusion nozzle from the filament feed motor with a flexible tube. This allows the printhead to be just 25mm in diameter and significantly reduces toolhead inertia, but requires more careful tuning of print parameters due to compressibility of the filament inside the tube.

4.1.1 DeltaXY Design Parameters. We created Fab Unit before the design tool of Sec. 8 was developed, and used a combination of

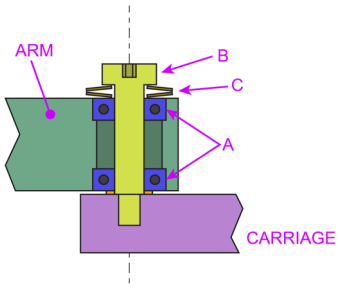

Figure 11: A shoulder joint design that utilizes a pair of radial bearings (A) running on a shoulder screw (B) and preloaded using disc washers (C). This design uses fewer parts but is estimated to be significantly less stiff for the same outer shoulder diameter.

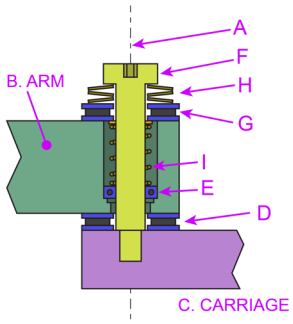

Figure 12: Fab Unit's shoulder joint rotates about axis A, absorbing radial and pitch moments between the arm (B) and carriage (C) by means of a thrust bearing (D) and a radial bearing (E) running on a shoulder screw (F). Preload is achieved through a top thrust bearing (G), disc washers (H), and a coil spring (I).

analysis spreadsheets and constraint-based sketch tools to arrive at a DeltaXY mechanism design. The width of Fab Unit was driven by the size of our chosen stepper motors and linear bearings. We selected NEMA17 motors because of their widespread use in 3D printers, compatibility with common driver electronics, and availability in many configurations, providing future flexibility. Our linear bearing selection was driven by a vertical toolhead stiffness target of $0.1\frac{N}{\mu m}$ based on our prior machine design experience. These choices limited the minimum machine width to 127mm. We sought to maximize driveline separation S while accommodating 20mm diameter shoulders with 3.5mm of running clearance each, resulting in $S = 100$mm. Our choice of workspace (discussed in Sec. 4.3) and front margin ($M_F = 10$) then determined arm lengths ($L = 148.66$). A key discovery was that we could project the shoulders in front of the linear bearings by extending the carriage plates. This allowed the use of shorter arms to decrease the ratio of $\frac{L}{S}$ and improve positioning resolution and lateral rigidity. The DeltaXY reference design of Figure 5 reflects Fab Unit's geometry, although for simplicity the workspace is illustrated as a rectangular subset.

4.1.2 Revolute Joints. A practical challenge of designing Fab Unit was the detailed architecture of DeltaXY's revolute joints. Because the printhead is cantelivered on the end of 149mm-long arms, its vertical rigidity is significantly influenced by the pitch moment stiffness of the shoulders. At the same time, we sought to minimize shoulder diameter to maximize driveline separation and performance. We started with a traditional joint design shown in Figure 11, which utilizes a pair of spring-preloaded radial ball bearings running on a shoulder screw. This configuration had the advantage of simplicity, with a shoulder bolt screwed directly into the carriage. However, based on first-order analyses, we were unable to achieve our target stiffness in an overall shoulder diameter of 20mm, due to closely spaced small-diameter bearings and flex in the shoulder bolt. We instead implemented the design shown in Figure 12, which absorbs pitch moments using a larger needle thrust bearing (Fig. 12G) sandwiched between the arm and carriage by a significant (~250N) preload force delivered through disc springs. A small radial ball bearing is used to absorb radial loads on the joint, which we lightly preload to eliminate play. As implemented, we estimate that the latter design is six times stiffer than the former at the printhead.

Figure 13 illustrates our design for the toolhead pivot. This joint is subject to radial loads, which are absorbed through a preloaded radial ball bearing. A key challenge here is minimizing the joint diameter while providing enough space for the toolhead to mount concentrically with the axis of rotation. Fab Unit's small extrusion nozzle mounts to a threaded hole inside the shaft that connects both arms, with the filament guide tube extending through the top end of the joint. Alternative joint designs may be needed for other toolheads, or the mechanism design might be modified to offset the toolhead from the pivot joint. This latter approach is later discussed in Section 6.

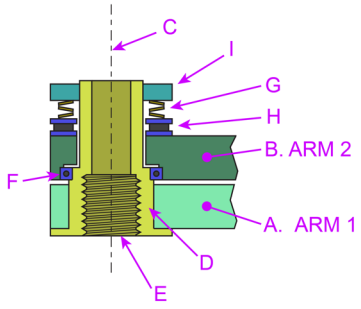

Figure 13: Fab Unit's toolhead pivot joint joins Arm 1 (A) to Arm 2 (B) while allowing rotation about axis C. It consists of a central shaft (D) with threaded tool mount (E), which is fixed to Arm 1. A ball bearing (F) couples the shaft to Arm 2, and is preloaded through disc washers (G), a thrust bearing (H) and a shaft collar (I).

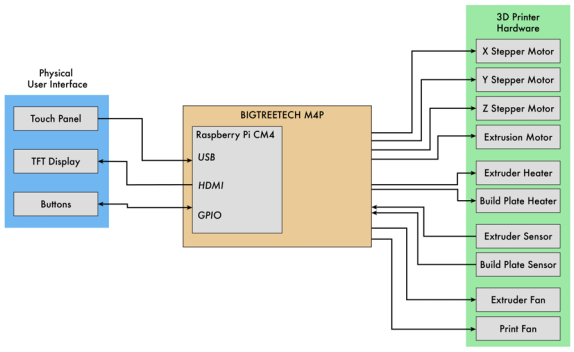

Figure 14: Fab Unit Electronics

4.2 Electronics and Control System

We envisioned Fab Unit as a self-contained device that could serve as a future testbed for on-tool interactions. We therefore built its control system (shown in Fig. 14) around an embedded Linux system running on a Raspberry Pi CM4 System-on-Module (SOM) and housed on a BIGTREETECH Manta M4P carrier board [6], which supports future touchscreen-based UIs, onboard print processing pipelines, and a motion control system. We chose Klipper [41]—a popular 3D printing control system — as our motion controller because it is primarily Python-based and runs directly on the SOM, facilitating future flexibility. Interactions with Fab Unit are currently via a browser-based Fluidd GUI [11] that is served by the SOM, and accessed by a personal computer over Wi-Fi.

We contribute a DeltaXY kinematics module for Klipper that extends prior work on Deltesian kinematics by adding support for DeltaXY mechanisms with asymmetric arm lengths and offset toolheads. This scaffolds future work (described in Sec. 6), and is important for calibration when the toolhead is not perfectly located on the pivot shaft axis because of manufacturing and assembly errors.

4.3 Workspace

Fab Unit was initially designed for printing small parts from a curated catalog. We designed the workspace around a 120x120mm build plate assembly, chosen based on commercial availability and our application requirements. With foreknowledge of our target set of printed parts, we were able to reduce machine depth and mechanism non-linearity by designing the mechanism to cover 92% of the build plate by excluding the front-most corners (illustrated in Fig 15). These types of optimizations are afforded by the shape of the DeltaXY work envelope, but for general-purpose use makes it difficult to easily answer the question "will my part fit?"

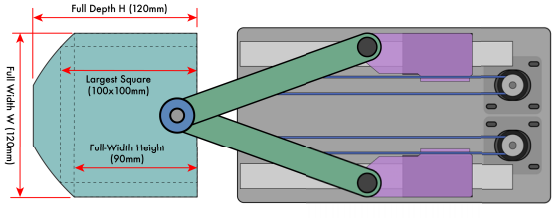

Figure 15: Fab Unit's Workspace

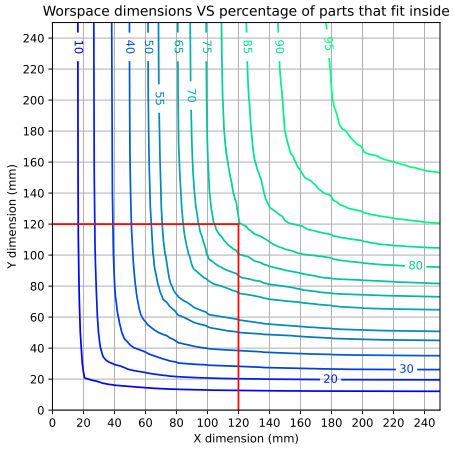

Figure 16: Percentage of parts that fit in a workspace of a given X and Y dimensions. This survey was conducted on 250k randomly selected files from Thingiverse. Each curve indicates the workspace needed to achieve a specific percentile. The red lines correspond to the full size of the Fab Unit's workspace, reaching the 80th percentile.

As later shown in Section 7.3 and Figure 26, workspace dimensions and machine depth are coupled, and available shelf depth limits workspace size. To help guide future development of rackable 3D printers, and to understand workspace capabilities of Fab Unit as a general-purpose printer, we conducted a survey of 250k randomly selected STL files stored on Thingiverse, a popular online repository of user-generated 3D models. Figure 16 illustrates percentile curves on the distribution of XY part dimensions, and can be used to guide the sizing of workspaces. For example, we found that Fab Unit's 120x120mm build plate can accommodate approximately 77.7% of the parts on Thingiverse. To understand the effects of the clipped corners on this metric, we found the set of parts whose

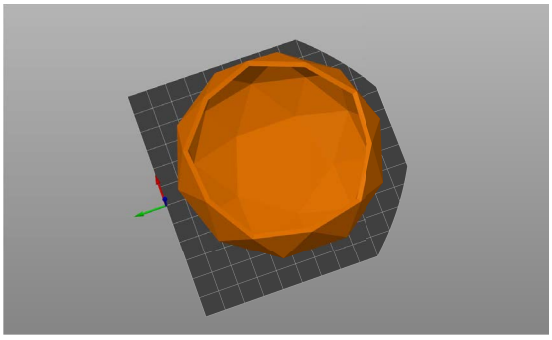

Figure 17: Round part fitting in the clipped worspace

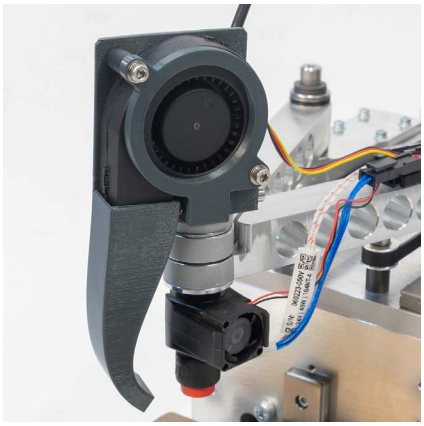

A. Cooling fan

B. Gear

C. 3DBenchy

Figure 18: A) Implementation of a part cooling fan. B), C) 3D printed parts produced by the machine.

dimensions fit within a square workspace of 120x120mm, but do not fit within a rectangle of 120x90mm; we took a random sample of 60 and manually plated them on our clipped build area, and found that 80% of these did indeed fit, often because they were circular, as illustrated in Fig. 17. We estimate Fab Unit's clipped build area can accommodate 76.7% of the Thingiverse database — a reduction of just 1%!

4.4 Print Results

The DeltaXY mechanism presents unique challenges when used in the context of 3D printing. The amount of airflow applied on the printed part is known to greatly affect its quality [28], but adding a cooling fan on the DeltaXY's toolhead must be done with careful consideration to not impact the minimum LSE of the machine (see Sec. 2.4). Figure 18 shows our implementation of a joint-mounted cooling fan and its effect on printing quality. The 3DBenchy [40] (a popular 3D printing benchmark model) in Figure 18C was printed in 61 minutes, which matches an equivalent print on an UltiMaker S3 [71] using default slicer settings.

Another challenge specific to DeltaXY is the distortion that can occur when the hotend is not centered on the pivot. The next section discusses this effect in detail and offers a calibration procedure to compensate for it. Figure 19 offers a comparison of the distortion before and after calibration of the toolhead offset. We measured this offset to be 1.8mm along X, and 3.3mm along Y.

An additional effect we observed during printing is the presence of backlash when reversing direction in the X axis. This is attributed to backlash in the belts and was measured to impact the dimension of the print by less than 0.1mm, which is typical accuracy for FDM parts [21]. Note that like actuator resolution, actuator backlash is amplified at the toolhead by the resolution gain G_R (see Sec. 7.5).

4.5 Calibration

The kinematics presented in Section 3.2 assume an ideal mechanism of known dimensions. In practice, various sources of errors during fabrication and assembly can contribute to uncertainty in the linkage parameters. In our experiments, the length of the arms and the placement of the shoulders were not found to be sources of error, as these parts were fabricated with precise numerical control. The main source of error was identified as an offset of the toolhead relative to its joint. We attribute this to a slight non-perpendicularity relative to the arms, amplified over the length of the printhead.

The effect of a toolhead offset can be simulated, offering a framework for identifying and correcting distortions observed in 3D printed parts. Figure 19A-D illustrates the distortions that would result from an exaggerated amount of offset in the X or Y direction. The effects are separable and distinct. The main effect of an offset along the X-axis is a skew of the Y-coordinate, causing parts to be compressed along one diagonal and elongated along the other. In contrast, an offset along the Y-axis causes compression or elongation along the X-axis.

A kinematic model that includes toolhead offset is presented in Appendix A. This model is used to control the machine once the offset has been calibrated. This consists of two steps, illustrated in Figures 19E and 19F. First, the Y offset is estimated by measuring the difference between the X and Y dimensions of a printed square. The Y offset is then applied, and a disk is printed. The X offset causes the disk to adopt an ellipsoid shape, as illustrated in Figure 19A. A measurement of its major and minor axes provides an estimate of the X offset. Once an initial estimate for both offsets is known, they can be fine-tuned together using the distortion model to account for the mutual residuals. A practical example of distortion is shown in Figure 19G, and the final result after calibration can be seen in Figure 19H.

4.6 Ergonomics and Scalability

We place Fab Unit's filament spool in the natural void formed below the horizontal DeltaXY baseplate and behind the vertical front plate supporting the Z axis. This makes Fab Unit entirely self-contained aside from power, and supports its goal of occupying minimal shelf space. However, it surfaces a constraint of rackable digital fabrication: minimal frontal space limits opportunities for control

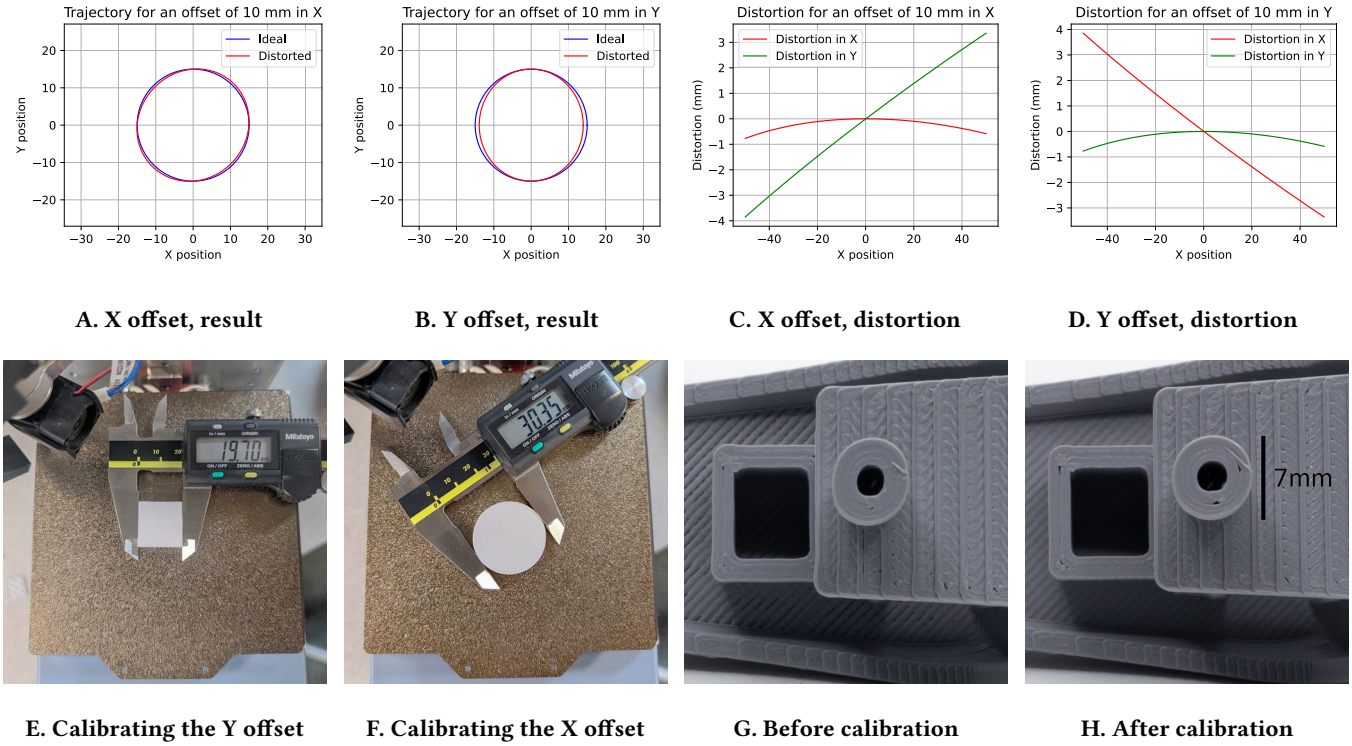

A. X offset, result **B. Y offset, result** **C. X offset, distortion** **D. Y offset, distortion**

E. Calibrating the Y offset **F. Calibrating the X offset** **G. Before calibration** **H. After calibration**

Figure 19: Top row: simulation of the distortion resulting from an offset in the toolhead's XY position relative to the joint. Bottom row: overview of the calibration procedure. E) A square is printed to estimate the compression due to the Y offset. F) After compensating for the Y offset, a disk is printed to estimate the skew caused by the X offset. G), H) 3D printed object before and after calibration.

surfaces and access panels. We anecdotally found that removing Fab Unit from a shelf to replace the filament spool was not too onerous, but quick release features on the side access panel would be beneficial.

Fab Unit is constructed using key components that are quite similar to those found on low-cost FDM 3D printers like the Bambu A1 Mini [26] — including similar types and quantities of linear bearings and actuators — which at the time of writing retails for $200 USD fully assembled. The DeltaXY mechanism requires additional low-cost commodity components to implement the shoulder joints, such radial and thrust bearings and disc washers. We spent approximately $1200 USD on components for our prototype, not including raw materials and any fabrication costs. Key components such as linear bearings and motors were sourced from manufacturers that primarily service the automation industry. A full bill of materials for the Fab Unit prototype is available online[5].

5 Interaction Opportunities for Rackable Digital Fabrication

We are motivated by the belief that a closer physical integration of digital fabrication into our living and working spaces can play an important role in inspiring how we might interact with and benefit from these exciting technologies in the future. To this end, we identify the narrow and deep *rackable digital fabrication* form factor as an alternative to desktop formats that expands where digital fabrication can be physically placed, and we contribute concrete design knowledge necessary to realize these architectures. Our Cantilevered DeltaXY mechanism allows very high lateral spatial efficiencies (LSEs) to be achieved *for small workspace dimensions*, enabling exceptionally narrow machine form factors.

We see this work as a springboard for HCI explorations that draw inspiration from alternative physical placement opportunities to develop new tools and interactions. In this section, we share three exploratory directions emerging from our early experiences developing and thinking about rackable digital fabrication tools. First, compact form factors that support inconspicuous digital fabrication may lead to physically ubiquitous digital fabrication, thereby stimulating the development of specialized tools for specific, location-dependent contexts of use, and suggesting interaction approaches that occur at-tool rather than at-computer. Second, rackable digital fabrication could make print farms more space-efficient, re-contextualizing them in homes, mobile "maker carts" [35], and library shelves. Third, shelf-born modular "personal factories" may become more practical and accessible, allowing individuals to compose and sequence heterogeneous fabrication processes to build complex objects. We expand on these visions in the following subsections.

[5]http://www.deltaxy.org

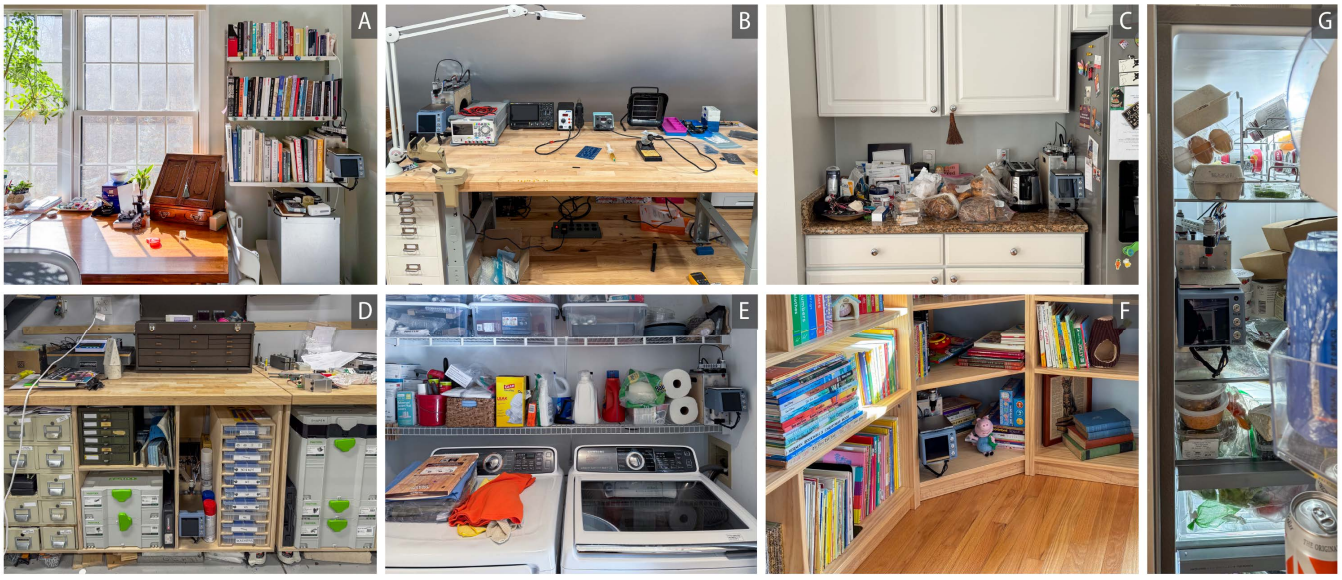

Figure 20: Rackable digital fabrication machines such as Fab Unit can inconspicuously fit into home and workshop settings including: A) a bookshelf adjacent to where mechanical design activities occur, B) an electronics workbench, C) a kitchen side counter, D) a metal and woodworking shop, E) a laundry room where odds and ends are stored, F) a children's bookshelf, G) inside a refrigerator.

5.1 Ubiquitous Fabrication

To help illustrate interaction opportunities afforded by compact rackable digital fabrication tools, we identified sites in the first author's home and workshop where Fab Unit (as a proxy for rackable fabrication tools in general) could be placed. Figure 20 shows possible placement options, ranging from immediately practical (the design space of Fig. 20A) to speculative (the refrigerator of Fig. 20G). The narrow, deep form factor of Fab Unit enables unique placement opportunities with minimal disruption to the surrounding environment; the images show how placing Fab Unit in diverse locations does not require significant restructuring of the current environment. In particular, rackable digital fabrication tools can take advantage of myriad narrow nooks, such as a gap between storage units (Fig 20D). Many storage spaces exhibit "compressibility" of their contents, which rackable form factors can readily use to their advantage. For example, fitting Fab Unit onto the laundry room rack of Fig. 20E did not involve removing any contents, but simply shifting them to the side. Our definition of "shelving" also encompasses *shelf-like* spaces. For example, the electronics bench in Fig. 20B and the kitchen side counter in Fig. 20 demonstrated an emergent organization where the front portion is active working space and the rear portion assumes a shelf-like function, with objects and equipment placed in a row.

Each location in Figure 20 suggests potential use-cases and interactions. Closest to current practice was placing Fab Unit on a bookshelf adjacent to the first author's desk (Fig.20A), where activities ranging from CAD to paying taxes occur. The author uses 3D printing as part of their design practice, but not regularly enough to justify significant space on their primary desk. Instead, their "desktop" FFF 3D printer is typically stored *under* a desk in the workshop and taken out when needed, introducing a sometimes disruptive distance between design and prototyping that is coherent with the findings of Annett et al.'s study of workshop environments [3]. Books on a shelf fit the same occasional usage pattern we describe with the 3D printer but are often conveniently placed nearby due to established storage patterns. We believe that a meaningful impact can be made on existing design practice simply by enabling digital fabrication tools to be placed closer to where design activities occur by fitting into existing storage systems, thus promoting lower activation energy for their use. Rackable digital fabrication provides an avenue for studying this connection, perhaps through a future interventional study that builds on Annett's observational work.

Other sites inspire *specific, context-dependent* use cases for digital fabrication. The electronics workbench (Fig. 20B) evokes questions of how 3D printing can support electronic prototyping practice, perhaps through on-demand production of components such as cable clips, board mounting hardware like standoffs and spacers, and accessories like potentiometer knobs. Specialized rackable digital fabrication tools for circuit board milling, solder paste deposition (see Sec. 8.2), and automated electronic testing (e.g. [30]) could be arranged like other test equipment at the back of the bench. Placing Fab Unit inconspicuously under a mechanical assembly bench near component and fastener storage (Fig. 20D) suggests a role for on-demand production of off-the-shelf mechanical components such as pulleys and gears. The kitchen environment of Fig. 20C suggests alternative form factors for food printing [49, 76] better able to integrate into existing spaces. The refrigerator context of Fig. 20G takes this to a speculative extreme, considering how rackable digital fabrication might extend existing appliances, for example to enable production of perishable objects. The kitchen

Figure 21: A) A university makerspace print farm that houses ~25 printers. B) A concept for a high-density mobile fabrication cart for education. C) A concept for micro print farms that might be distributed throughout public settings such as libraries.

side counter of Fig 20C also happens to be where keys and other knickknacks accumulate, indicating a high-traffic location that may be ideal for digital fabrication technologies designed to support daily life through everyday making [58]. Laundry rooms like the one shown in Fig. 20E sometimes double as pantries for household storage, and similarly might be amenable to on-demand production of household goods. Lastly, the children's room of Fig. 20F inspires educational applications for digital fabrication (designed with appropriate safety considerations for this audience), perhaps even tied to books living on the shelf. Many of the examples articulated above challenge existing notions of traditional digital fabrication as an output device for desktop computer-based design workflows, and instead point towards casual at-tool interactions that are more akin to kitchen appliances. We speculate that there is an underexplored interaction design space for walk-up-and-use *digital fabrication appliances*, and that rackable digital fabrication could provide fruitful physical contexts for such explorations.

5.2 Re-Contextualizing Print Farms

Print farms are centralized collections of 3D printers that serve a community, and are typically located in schools, independent makerspaces, and libraries. It is typical for a print farm to occupy an entire shelving unit or even room; for example, the academic makerspace print farm shown in Fig. 21A includes a room filled with floor-to-ceiling racks containing ~25 printers. This capacity is needed because the makerspace supports courses from more than 30 academic departments. We see opportunities for rackable form factors to impact who has access to digital fabrication as a common resource, and where they are able to engage with it. High lateral spatial efficiencies, coupled with the insight that many parts tend to be small (see Figure 16), imply that print farms such as in Fig. 21A could be designed to occupy significantly less space. For example, the UltiMaker S3 printers [71] currently employed in the print farm shown in Fig. 21A each occupy ~400mm of lateral shelf space. If the print farm's part size distribution mimics that of Thingiverse, then $\frac{4}{5}$ of those printers could be replaced by a machine similar to Fab Unit, which could reduce the size of the print farm by over 50%.[6] This has implications for how institutions are able to make digital fabrication capacity available to their communities, and thus for how digital fabrication plays a role in their community members' lives.

Beyond making *existing* print farms more space efficient, rackable digital fabrication opens a door to thinking about how print farms could take on new contexts. We envision *high density* mobile digital fabrication carts that can be brought to a classroom, as illustrated in Figure 21B. The cart in this rendering is 47" (1.2m)L x 20" (0.5m)W x 41" (1m)H in overall dimensions, and houses 14 Fab Unit 3D printers. This represents over 50% of the entire capacity of the print farm room of Fig. 21A, and could support many students at once. While each printbed size is significantly smaller, this is aligned with short-duration classroom activities. Such a cart might alternatively bear a heterogenous mix of rackable digital fabrication tools such as plotters, vinyl cutters, small milling machines, and laser cutters in addition to 3D printers, and could be modularly reconfigured based on curricular needs. This concept builds on McKay and Peppler's MakerCart concept [35], which is dimensionally larger and houses three machines that must be removed and set up before use. McKay and Peppler found that many schools do not have space for permanent makerspaces, and identify that mobile Fab Labs hold benefits for teacher exposure and curricular development by meeting teachers and students in their classrooms[35]. We believe that high density mobile fabrication carts could further these goals of digital fabrication literacy and also catalyze research into appropriate digital fabrication interfaces for educational settings.

We see opportunities for "micro" print farms that could be distributed within public spaces like a library (Fig. 21C) rather than placed in a central location. This may facilitate interactions that combine book-based research with digital fabrication, or promote interpersonal interactions sparked by seeing what other people are printing while browsing. These concepts are set against considerations regarding environmental health in public settings, including noise and fumes that may be generated by digital fabrication equipment. Micro print farms could also play a role in homes or small workshop. Many objects are made from assemblies of parts, and the ability to parallelize printing could significantly accelerate the speed with which multi-part objects can be created. For example,

[6] We assume the print farm went from 25 UltiMaker S3s (total width = 25×394mm = 9.8m) to 5 Ultimaker S3s and 20 rackable Fab Unit 3D printers (total width = 5×394mm + 20×127mm = 4.5m). We utilize Fab Unit's LSE of 94% rather than MLSE of 82%, as expected part size distributions should give flexibility in sharing space between machines by alternating assigment of smaller and larger parts. We do not account for how print times for larger parts affect the ideal distribution of printer sizes, which is nuanced when print farms are not serviced 24 hr/day.

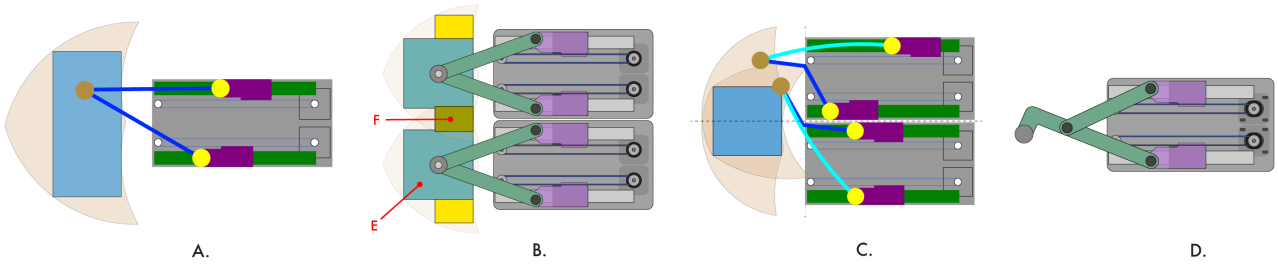

Figure 22: An array of adaptations of DeltaXY, including A) workspaces whose LSE is greater than the machine width, B) adjacent machines with primary (E) and shared secondary (F) workspaces, C) adjacent machines with completely overlapping workspaces and asymmetrical arms, and D) a mechanism with a toolhead that is offset from the central pivot axis.

a small three-part assembly could be fabricated thrice as fast by a micro print farm consisting of three Fab Unit devices than by a single UltiMaker S3, in an equivalent amount of shelf space. [7] This has implications for expanding the utility of 3D printing for everyday settings, where multi-part assemblies may be beneficial, and accelerating prototyping in space-constrained environments. It also affords opportunities for rapid small-run batch production.

We note Hudson et al.'s research from 2016, which found that beyond providing publicly available fabrication capacity, print farms (or "print centers") played a vital role in providing technical support to users [24]. When imagining print farms in contexts other than centralized, staffed facilities, these are considerations that should be kept in mind, while acknowledging improvements over the intervening decade to design software, print interfaces, and machine reliability.

5.3 Modular Personal Factories

Digital fabrication began as a factory-based technology, and has subsequently become accessible to individuals as desktop personal fabrication devices. Today, personal digital fabrication tools replicate discrete industrial processes, but not the organizational structure of automated machines as linked workflows. Rackable digital fabrication offers the potential to combine the functionality of machines in several ways to realize sub-industrial multi-process workflows. Because DeltaXY enables tools to reach past the extents of their chassis, adjacent machines may either partially or fully share workspaces. This could enable toolheads with different capabilities to operate on the same part without changing tools. We can also imagine a rack of digital fabrication tools enacting modular, pipelined processes, where workpieces transit between specialized machines. For example, a sub-industrial PCB production line might be realized by adjacent machines for PCB milling, solder paste deposition, part placement, and testing. Beyond traditional fabrication domains, fields such as biology research often apply multiple steps to process samples. Using biology research as a test-case, HCI researchers have explored how automated workflows can be flexibly customized through the use of computational notebooks and toolchanging machines [63]. Rackable digital fabrication offers the possibility to extend the application of computational notebooks to flexibly configure pipelined processes. In summary, sub-industrial "factories" enabled by rackable digital fabrication hold potential to open new possibilities for how users engage with digital fabrication tools and the design processes that drive them.

[7] We assume equivalent print speeds, which is supported by our initial testing.

6 Future Adaptations on the DeltaXY Mechanism

Over the course of developing DeltaXY, and considering the applications outlined in Section 5, we envision several mechanism adaptations that could enable new areas of HCI inquiry.

6.0.1 LSE > 100%. Fab Unit demonstrated an LSE slightly less that 100%. However, it is possible to create workspaces wider than the machine itself as illustrated in Figure 22A. This enables adjacent machines to partially share workspaces, allowing multiple machines to work on longer continuous workpieces, or to pass material between machines. For this latter use-case, one might inscribe primary and secondary rectangular working areas (Fig. 22E and F, respectively) within the same mechanism work envelope. Through an understanding of the design considerations provided in Section 7, researchers can design machines to take advantage of this unique capability of DeltaXY while still obtaining necessary performance.

6.0.2 Asymmetric Workspaces. Adjacent machines may entirely share a common workspace through the use of differing arm lengths, as shown in Figure 22C, which could enable multi-process fabrication without changing tools or transiting the workpiece. In some cases, this can also be used to speed work through parallelization. Asymmetric workspaces are supported by the design tool presented in the upcoming Section 8.

6.0.3 Offset Toolheads. The reference design for DeltaXY presented in Fig. 5 and embodied by Fab Unit places the toolhead concentric with the central pivot axis. This simplifies analysis, but can limit the range of toolheads accomodated by the mechanism. Offsetting of the toolhead is possible, as illustrated in Fig. 22D, and we provide the equations of motion for an offset Cantilevered DeltaXY mechanism in Appendix A.

6.0.4 Integrated Z Axis. To enable multiple machines to work on a single workpiece, it is advantageous for the toolheads to be independently actuated in the Z direction. We propose that one suitable

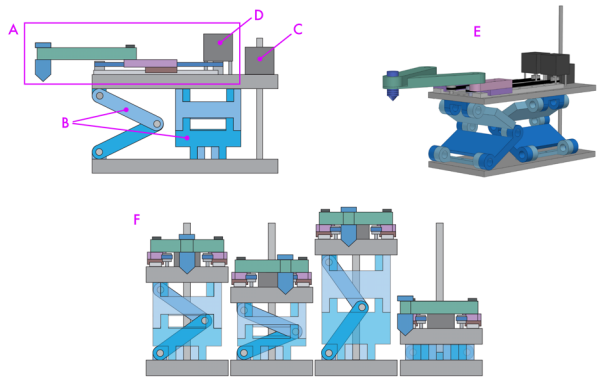

Figure 23: Applying a Sarrus linkage to actuate DeltaXY in the Z direction. A DeltaXY mechanism (A) is stabilized by two orthogonally oriented linkages (B) and actuated vertically by a non-captive stepper motor-driven leadscrew actuator (C). The DeltaXY drive motors (D) have been moved to the top. E) An isometric view of the Z-actuated DeltaXY mechanism. F) This mechanism permits adjacent machines to each independently move in 3 axes.

mechanism for this is the Sarrus linkage [19], shown in Fig. 23. This approach does not add width to the positioning mechanism, and can be actuated simply with a non-captive leadscrew motor (Fig. 23C). We are inspired by the work of Langford and Calish [27], and PavloG, who adapts the Sarrus linkage to lift and lower a build plate rather than the XY positioning mechanism [43].

6.0.5 Alternative Configurations. While the strong focus of this paper in on rackable fabrication, it bears mentioning that the cantilevered nature of DeltaXY enables configurations where multiple toolheads access the same work area from multiple sides, as shown in Fig. 24.

7 DeltaXY Guidebook

To support HCI researchers in exploring the design space of rackable digital fabrication, we propose a design process and first-order scaling laws for customizing DeltaXY to specific applications. A typical design might seek 100% or greater lateral spatial efficiency (LSE) with constraints on machine depth and performance targets for a given application (e.g. positioning resolution, rigidity, and acceleration). Because DeltaXY is kinematically non-linear, and has multiple coupled parameters, we have found the design process to be iterative. Figure 25 illustrates key aspects of the design parameter space for our reference design, and will be referred to throughout this section. The performance characteristics of DeltaXY's underlying kinematic chain has been rigorously analyzed [10, 31, 50, 74], and an analytical overview of PKM design considerations is given by Son et al. [61]. Here, we contribute first-order approaches that are well-matched to our design task and accessible to a wider range of practitioners. In the following analyses we assume linkage arms of equal length. Our design tool (Section 8) supports asymmetric configurations.

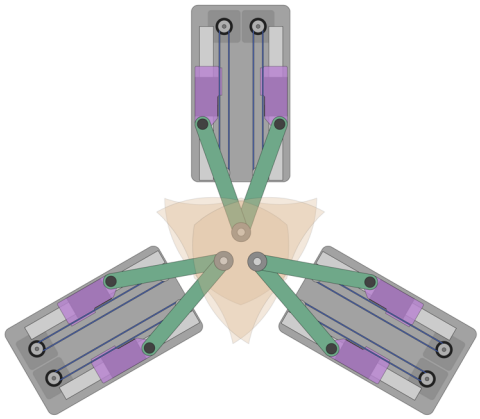

Figure 24: Because the workspace is cantilevered in front of the machine base, multiple DeltaXY machines can be oriented to share a common workspace. This exploration briefly steps outside our focus on rackable digital fabrication to show ancillary possibilities of afforded by the DeltaXY mechanism.

7.1 Workspace, LSE, and Machine Width

We start by defining a desired workspace of width W and height H (although non-rectangular workspaces are also possible). Based on an initial LSE target of 100%, we arrive at a target machine width $W_M = W$ using our definition of LSE:

$$LSE = \frac{W}{W_M} \qquad W_M = \frac{W}{LSE} \tag{1}$$

Two factors may limit W_M and LSE. First, the linear bearings, timing belt loop, and motors require a minimum lateral space. If the base becomes too narrow, the motors will interfere (Fig. 25A). This component selection is based on performance targets. Second, the toolhead has width $\varnothing_T$, and when $W + \varnothing_T > W_M$, the edge of the toolhead can protrude past the edge of the machine. In many situations this may be acceptable, and an advantage of DeltaXY over alternatives such as parallel SCARA (2E) is that the toolhead inherently leads the arms when outside machine bounds, limiting opportunities for interference with adjacent objects. Maximizing

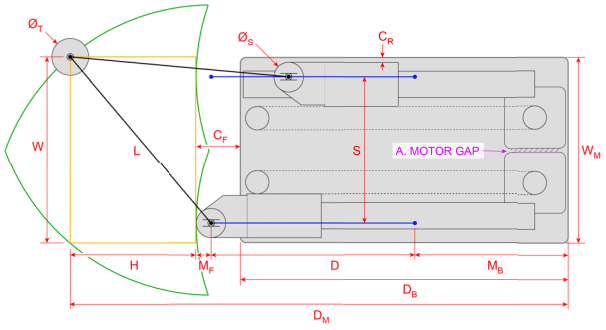

Figure 25: DeltaXY Workspaces and Machine Footprint

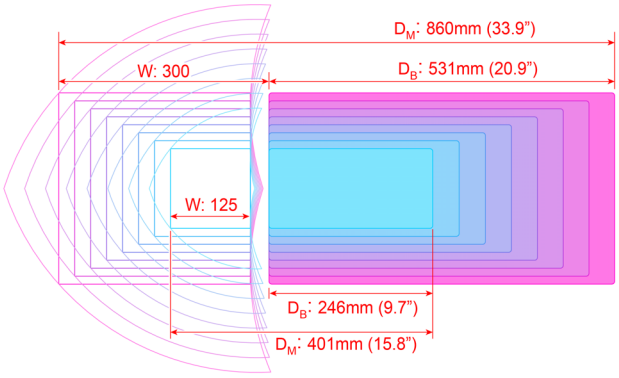

Figure 26: Example machine dimensions for square workspaces with an LSE of 100%

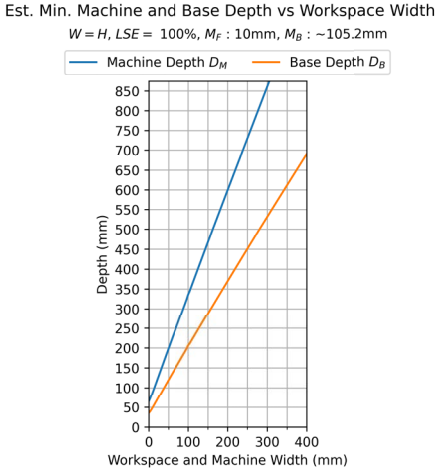

Figure 27: Base and machine depths for square workspaces with LSE = 100%. Assumes M_B from the reference design.

LSE and minimizing interference impact the rackability of a digital fabrication machine.

7.2 Linkage Parameters

Positioning resolution and rigidity improve by minimizing the ratio of arm length L to driveline separation S, suggesting we should aim to maximize S. For a fixed based width W_M, S_{max} is limited by the shoulder diameter $\varnothing_S$ (which influences toolhead rigidity) and the shoulders' running clearance C_R to the edge of the base:

$$S_{max} = W_M - \varnothing_S - 2C_R \tag{2}$$

With S fixed, link length L can be determined graphically as shown in Figure 25. We can make L shorter by decreasing the front margin M_F, which projects the shoulders further ahead of the linear bearing blocks; however, past a certain point this impacts dynamic performance and Z-axis rigidity. Driveline length D is found by moving the toolhead to the back edge of the workspace with one arm horizontal; that arm's shoulder is at the driveline endpoint. These parameters are given by:

$$L = \sqrt{\left(\frac{S}{2} + \frac{W}{2}\right)^2 + (H + M_F)^2} \tag{3}$$

$$D = L - M_F \tag{4}$$

7.3 Machine Depth

The DeltaXY mechanism enables rackable digital fabrication machines to achieve a high LSE by sacrificing depth — an affordance of shelf living. However, available shelf depth *is* finite and constrains the machine design. Overall machine depth D_M considers the distance from the front of the workspace to the back of the base. Base depth D_B is the depth of the fixed machine base; in some cases, it may be acceptable for the front of the machine to hang over the edge of a shelf, as long as the base is fully planted. The overall depth is given by:

$$D_M = H + M_F + D + M_B \tag{5}$$

where M_B is a *back margin* between the driveline terminus and the back edge of the machine. M_B can exceed the driveline length, and incorporates mechanical overheads such as: bearing truck lengths, excess rail length, drive motors, and machine-specific elements including extrusion motors, electronics, etc. M_B also captures *front clearance* C_F, which provides operating space for the toolhead radius ($\frac{\varnothing_T}{2}$) between the back edge of the workspace and the front of the base. Figures 26 and 27 provide first-order insight into possible depth requirements of DeltaXY by illustrating how machine depth can vary with workspace width [8].

7.4 Kinematic Equations

In subsequent sub-sections, we provide scaling laws and first-order analyses to inform the design of DeltaXY based on performance considerations. These are derived from equations governing the motion of the mechanism. Inverse kinematic equations relate the toolhead position (X_T, Y_T) to shoulder positions Y_1, Y_2:

$$Y_1 = \sqrt{L^2 - \left(\frac{S}{2} - X_T\right)^2} + Y_T \tag{6}$$

$$Y_2 = \sqrt{L^2 - \left(\frac{S}{2} + X_T\right)^2} + Y_T \tag{7}$$

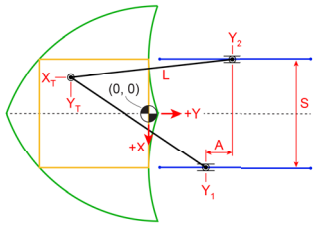

Figure 28: Coordinate frame used for kinematic equations

[8] $\varnothing_S$ and truck length are scaled according to [59] for increasing stiffness requirements as L increases, with a proportionally minor effect on mechanism dimensions.

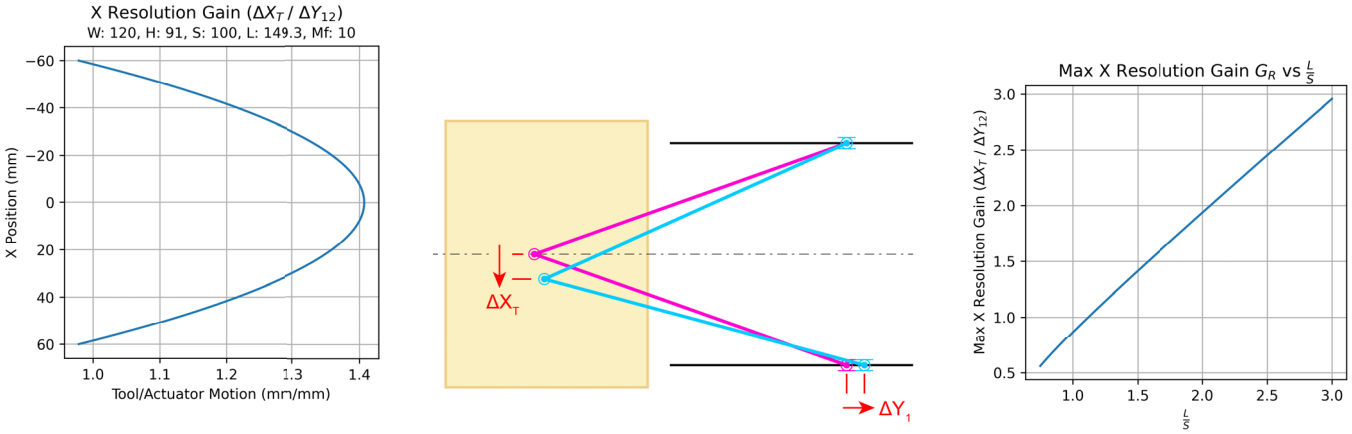

A. Resolution gain over workspace for the reference design of Fig. 5

B. Actuator amplification in X

C. G_{Rmax} grows with $\frac{L}{S}$

Figure 29: DeltaXY Positioning Resolution

Forward kinematic equations relate shoulder positions to the toolhead position:

$$A = Y_2 - Y_1 \tag{8}$$

$$X_T = L \sin\left(\frac{\pi}{2} - \tan^{-1}\left(\frac{A}{S}\right) - \cos^{-1}\left(\frac{\sqrt{A^2+S^2}}{2L}\right)\right) - \frac{S}{2} \tag{9}$$

$$Y_T = Y_1 - L\cos\left(\frac{\pi}{2} - \tan^{-1}\left(\frac{A}{S}\right) - \cos^{-1}\left(\frac{\sqrt{A^2+S^2}}{2L}\right)\right) \tag{10}$$

These kinematic equations adopt the coordinate system illustrated in Figure 28.

7.5 Positioning Resolution

DeltaXY has a constant Y-axis toolhead positioning resolution ΔY_T that is equal to the actuator resolution ΔY_{12}, and is achieved when both shoulders move equally $\Delta Y_1 = \Delta Y_2 = \Delta Y_{12}$. In the X direction, differential actuator motion is amplified or attenuated at the toolhead by a gain factor G_R (illustrated in Fig. 29B) such that the X-axis toolhead positioning resolution $\Delta X_T = G_R \cdot \Delta Y_{12}$. We find G_R by differentiating Eq. (9) with respect to A (i.e. $Y_2 - Y_1$). Figure 29A shows this gain factor across the workspace of the reference mechanism of Fig. 5. Worst-case resolution gain G_{Rmax} occurs at $X = 0$, and improves as $\frac{L}{S}$ decreases (see Fig. 29C):

$$G_{Rmax} = \frac{\Delta X_T}{\Delta Y_{12}} = \sqrt{\frac{L^2}{S^2} - \frac{1}{4}} \tag{11}$$

$$\frac{L}{S} \leq \sqrt{\left(\frac{\Delta X_{Tmax}}{\Delta Y_{12}}\right)^2 + \frac{1}{4}} \tag{12}$$

Eq. (12) provides a maximum ratio of $\frac{L}{S}$ for a target resolution $\Delta X_T = \Delta X_{Tmax}$. For our reference design, actuator resolution is dependent on step size, driver microstepping [17], and pulley pitch diameter.

7.6 Lateral (XY) Rigidity

Stiffness of a positioning mechanism relates toolhead forces F to deflection δ through $K = \frac{F}{\delta}$. Its inverse is compliance $C = \frac{\delta}{F}$. As with resolution, DeltaXY exhibits a lateral *compliance gain* G_C that amplifies actuator (motor + belt) compliance C_{12} at the toolhead ($C_{tool} = G_C \cdot C_{12}$); drivetrain components tend to be the "softest" parts of the system and dominate overall lateral system compliance. Fig. 30A graphs this gain across the workspace of our reference mechanism. Maximum G_C (G_{Cmax}) occurs in the X direction at the mechanism midline, and through a force and moment balance and geometric analysis of Fig. 30B is found to be:

$$G_{Cmax} = \frac{C_{max}}{C_{12}} = 2\frac{L^2}{S^2} - \frac{1}{2} \tag{13}$$

$$\frac{L}{S} \leq \frac{\sqrt{2}}{2}\sqrt{\left(\frac{C_{max}}{C_{12}}\right)^2 + \frac{1}{2}} \tag{14}$$

This analysis is valid for $G_{Cmax} > 1$ (or $\frac{L}{S} >\sim 0.866$); below these values, compliance in the Y direction begins to dominate. Figure 30C shows how G_{Cmax} scales with $\frac{L}{S}$. **DeltaXY's lateral stiffness quickly worsens as $\frac{L}{S}$ grows, establishing practical design limitations.** Eq. (14) provides a maximum ratio of $\frac{L}{S}$ for a target maximum toolhead compliance of C_{max}. Actuator compliance C_{12} can be estimated by summing belt drive and stepper-motor compliances, using approximations provided by Perneder's *Handbook Timing Belts* [47, pp.78-84, 170-175] and Acarnley's *Stepping Motors: A Guide to Theory and Practice* [1, pp.25-29], respectively. Belt drives have a variable compliance depending on position, with maximum compliance (i.e. mininum stiffness) when the carriage is furthest from the drive pulley. DeltaXY has a minimum lateral stiffness along the midline at the furthest edge of the workspace, as shown in Fig. 30B.

7.7 Z Axis Rigidity

Orthogonal (Z-axis) toolhead compliance is found by summing toolhead compliances:

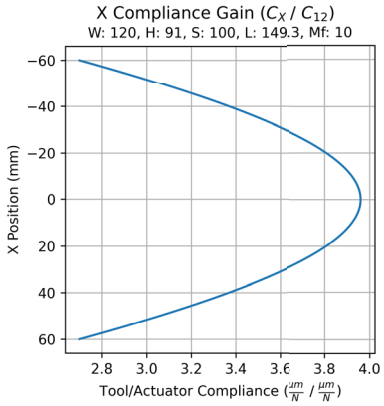

A. Compliance gain over workspace for the reference design of Fig. 5

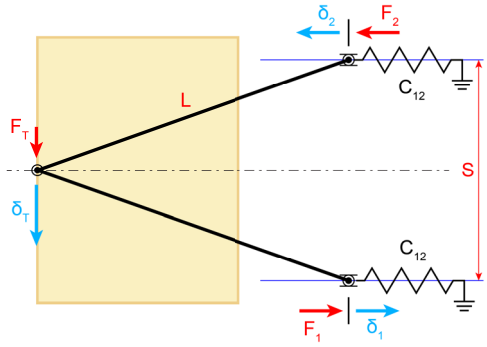

B. Compliance amplification in X

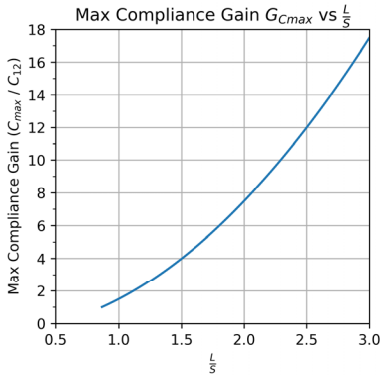

C. G_{Cmax} grows as $\left(\frac{L}{S}\right)^2$

Figure 30: DeltaXY Lateral (XY) Compliance

- Arm compliance can estimated using beam bending theory or finite element analysis (FEA), and scales with L^3.
- Pitch compliance of the shoulders. A first-order estimate for bearing pitch stiffness is provided by Slocum [59, pp.10-22 – 10-23].
- Pitch compliance of the linear bearing trucks. These can be estimated using formulas provided by Slocum [59, pp. 10-23], or obtained from the bearing manufacturer.

Figure 31 illustrates how these compliances combine to affect Z-axis toolhead stiffness. Arm cross-sections can be increased to benefit overall Z-axis stiffness, but if material is added, greater moving mass will negatively affect dynamic performance (see upcoming Section 7.8). Larger bearing diameters can also significantly improve Z-axis stiffness but may reduce driveline separation S (see Eq. 2) to the detriment of resolution and lateral compliance. A typical design approach balances the compliance contributions of all elements [60, p. 43] to avoid over-design at the cost of overall system performance.

7.8 Dynamic Performance

The DeltaXY mechanism has several sources of inertia that must accelerate with the toolhead, illustrated in Fig. 32. As the tool moves laterally across the workspace, the relationship between its motion and that of each inertial element changes. Ignoring compliance and friction effects, we estimate the acceleration capability of the mechanism through a position-dependent *acceleration gain* G_A that relates toolhead acceleration A_T to actuator force F_{12}:

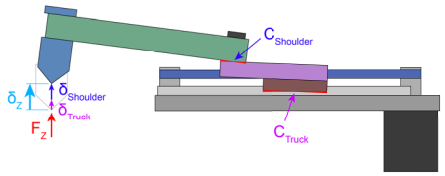

Figure 31: Z Compliance

$$G_A = \frac{A_T}{F_{12}} \tag{15}$$

We can estimate G_A by first reflecting the mass of each inertial element to the toolhead, using the well-known equation [33]:

$$m_i = \frac{J_i}{n_i^2} \tag{16}$$

where J_i is a generalized component inertia, m_i is the component inertia reflected at the toolhead, and n_i is the transmission ratio that relates translational toolhead velocity V_T to translational or rotational component velocity V_i through $n_i = \frac{V_T}{V_i}$. To obtain the total reflected inertia at the toolhead, we sum the individual reflected inertial components:

$$m_{total} = M_T + \frac{M_A}{n_{MA}{}^2} + \frac{J_A}{n_{JA}{}^2} + \frac{M_C}{n_{MC}{}^2} + \frac{M_B}{n_{MB}{}^2} + \frac{J_M}{n_{JM}{}^2} \tag{17}$$

where M_T is toolhead mass, M_A is arm mass, J_A is arm rotational inertia, M_C is carriage mass, M_B is bearing mass, and J_M is motor inertia. Eq. (17) only represents one side of the mechanism, and in practice both arms, carriages, bearings, and motors should be included. To calculate the acceleration gain from this reflected mass, we take its reciprocal and additionally divide by the resolution gain

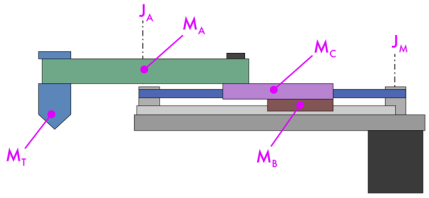

Figure 32: DeltaXY inertia is comprised of toolhead mass M_T, arm mass M_A, arm rotational inertia J_A, carriage mass M_C, linear bearing mass M_B, and motor rotational inertia J_M

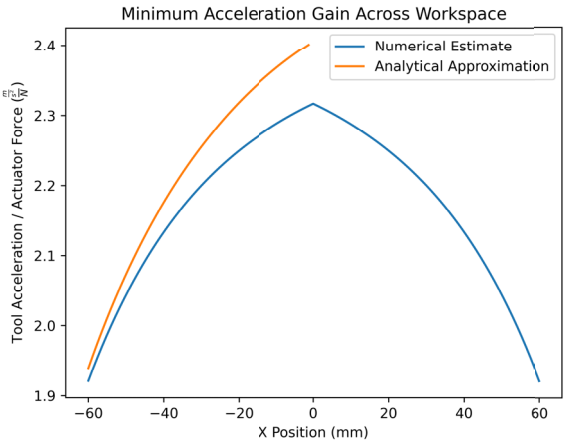

Figure 33: Estimated acceleration gain for Fab Unit based on toolhead mass and effective actuator inertia.

factor G_R found in Sec. 7.5 to account for force attenuation from the actuator to the toolhead:

$$G_A = \frac{1}{m_{total}} \cdot \frac{1}{G_R} \tag{18}$$

We define an alternative metric of *effective mass* (m_{eff}) which is the reciprocal of the acceleration gain ($m_{eff} = \frac{1}{G_A}$) and is useful because it can be decomposed into a sum of constituent components representing each inertial element. This helps target primary areas for improving dynamic performance through inertia reduction, and is the metric we utilize in the DeltaXY design tool of Section 8.

The scalar velocity relationships n_c between toolhead motion and each component vary with the toolhead's lateral position, as well as the direction of motion. To determine the worst-case acceleration gain at each point in X travel, we've found it most useful to reframe Eq. (17) as a sum of matrix multiplications, where n_c becomes a Jacobian[9]. Figure 33 illustrates this worst-case acceleration gain for Fab Unit, ignoring arm inertias. Acceleration performance drops towards the periphery of the workspace, because the effective actuator mass ($M_{act} = M_C + M_B + J_{M-reflected}$) dominates, as the actuator must travel further for a given toolhead motion. We have found that the following first-order estimate provides reasonable values for G_A when toolhead mass is low (in this case 100g) relative to effective actuator mass, but diverges in the center of the workspace as the toolhead becomes heavier:

$$G_A = \frac{1}{GM_T + \frac{1}{G}M_{act}} \tag{19}$$

where:

$$G = \sqrt{\left(\frac{dY_1}{dX_T}\right)^2 + 1} = \frac{\sqrt{4L^2 - (S - 2X)^2}}{2L} \tag{20}$$

This estimate is graphed alongside computed values in Fig. 33.

[9]See Eq. (39) in Liu et al., which is provided as part of a more sophisticated analysis [31].

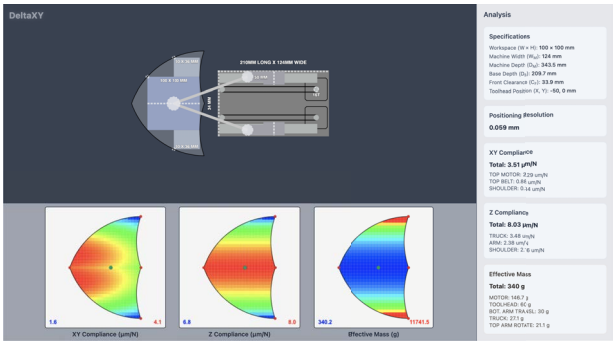

Figure 34: The DeltaXY design tool. Top-left: an interactive machine model whose linkage parameters can be adjusted by dragging. Bottom-left: heatmaps of XY compliance, Z compliance, and effective mass across the workspace. Right: real-time analytics including overall dimensions and toolhead positioning resolution.

8 Design Tool

8.1 Overview

To support exploration of the DeltaXY mechanism and to assist in developing new machines based on its kinematic architecture, we created a browser-based design tool. The tool allows users to interactively reconfigure the mechanism by dragging linkage elements, with parameter updates in real time. Manipulable features in the design tool are denoted with dashed elements. A screenshot is shown in Figure 34.

The design tool provides live analytics of the current configuration, including overall machine specifications (workspace size, depth, clearance), positioning resolution, and performance metrics such as XY compliance, Z compliance, and effective mass. Each metric is further broken down into contributing factors (e.g., motors, belts, arms, and joints), giving insight into how component-level choices shape overall performance.

Behind these outputs, the tool implements mechanical analysis algorithms that solve both forward and inverse kinematics for the parallel linkage, compute compliance from belt stiffness, bearing deflections, and arm bending (via beam theory), and estimate equivalent mass including translational and rotational inertia effects. These calculations are performed in real time, with heatmap generation offloaded to web workers to maintain responsiveness while preserving engineering accuracy.

Workspace performance is visualized through three heatmaps of XY compliance, Z compliance, and effective mass (log-scaled), making the non-linear characteristics of the mechanism immediately apparent. The heatmaps draw on detailed component specifications, including material properties, bearing selection, belt stiffness, and motor resolution. Designers can also specify a target workspace, and the tool automatically derives required linkage dimensions and evaluates boundary performance.

The tool complements the analysis presented earlier in Section 7 by making first-order scaling laws and heuristics directly explorable. Instead of requiring manual derivation or spreadsheet calculations, the relationships are encoded into an interactive form

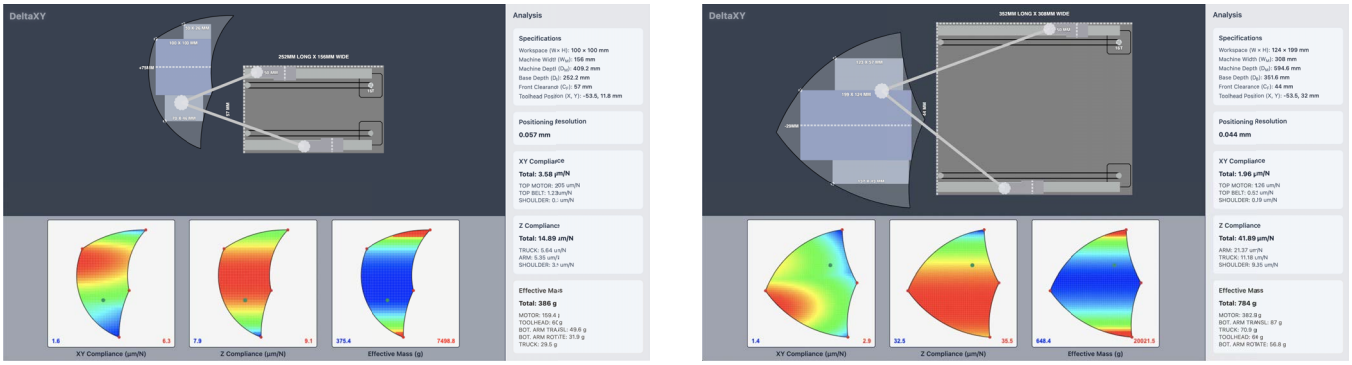

Figure 35: The DeltaXY design tool in two alternative configurations.

where changes to linkage parameters immediately reveal their impact on workspace and performance. This provides a means for others to extend DeltaXY to new machine architectures. Heatmaps make non-linearities visible at a glance, and side-by-side configurations (Figure 35) allow rapid comparison of trade-offs. The tool offers an entry point for exploring the design space of rackable digital fabrication systems.

The DeltaXY design tool software and source code is accessible online under a non-commercial open-source license[10].

8.2 Workflow

To illustrate how the DeltaXY design tool can support machine designers to realize rackable digital fabrication form factors, we walk through a hypothetical design process. Our protagonist Barbara often prototypes printed circuit boards (PCBs), and has grown tired of manually soldering small components. She is interested in applying reflow techniques, but does not want the cost and hassle of working with solder paste stencils. Barbara sees a need for a compact, automated syringe-based solder paste dispenser that can sit alongside other tools at the back of her electronics workbench, and identifies this as a good application for the DeltaXY mechanism. She outlines design goals and constraints for the machine:

- Reaches anywhere on a 100x150mm PCB, based on limits imposed by her free circuit layout software.
- Achieves a positioning resolution of 50um, which is 10x smaller than a 0.5mm pitch QFN package.
- Maximizes working speed by minimizing moving inertia.
- Treats mechanism stiffness as a secondary concern because contact forces are estimated to be quite low (<0.1N).
- Only needs to actuate a few mm in the Z direction.

Barbara opens the DeltaXY design tool, and performs the following steps:

(1) Barbara resizes the primary workspace to 150x100mm, by dragging its upper left corner (Fig. 36A). She observes that the resultant positioning resolution is too large at 80um.
(2) She selects a motor with half the step size in the settings menu (Fig. 36B). Now the resolution is 40um, and below her upper limit.
(3) Barbara begins experimenting with the machine width by dragging the base plate's upper edge, exploring how narrow she can go. She immediately notices that machine widths less than 127mm cause the motors to interfere (Fig. 36C).
(4) Seeing plenty of headroom in the compliance values, she tries selecting narrower (and less stiff) bearings. This allows her to reduce machine width to 117mm, and positioning resolution gets slightly worst (Fig. 36D).
(5) Barbara has a radical idea. What if she were to allow the motors to overlap by mounting them from both sides of the base plate, and stacking the belts on top of each other? She quickly tries this to see how positioning resolution is affected (Fig. 36E). Resolution jumps to 76um.
(6) She plays with the gap between the workspace and the machine base, as well as the projection of the shoulders ahead of the bearing trucks. The positioning resolution improves to 59um (Fig. 36F).
(7) Barbara discovers that smaller timing belt pulleys are available, and changes the tooth count from 20T to 16T by dragging the pulley diameter (Fig. 37A). This lands the positioning resolution at 48um, which is under her goal! While effective mass increased by about 14%, Barbara decides that an extremely narrow machine width of just 74mm is worth a fractional loss in dynamic performance.
(8) Barbara does a quick sanity check by dragging the toolhead around the workspace, paying attention to the heat maps and readouts to see if anything looks concerning along the range of motion.
(9) Satisfied with her initial design, Barbara uses the parameters she discovered to guide her CAD process and create a rough 3D model. She anticipates iteratively consulting the design tool throughout the detailed design process in response to unforeseen challenges.

Figure 37B shows the resulting rough CAD model . Barbara's initial design achieves an LSE of over 200%, showing promise for a final concept that will compactly occupy desk space when in storage, and can be brought forward into the active portion of her workbench when in use. This use pattern raises interaction questions such as whether her solder paste dispenser is driven by a file exported from CAD, or perhaps uses computer vision to identify pre-tinned pads on the PCB and apply paste without any

[10]http://www.deltaxy.org

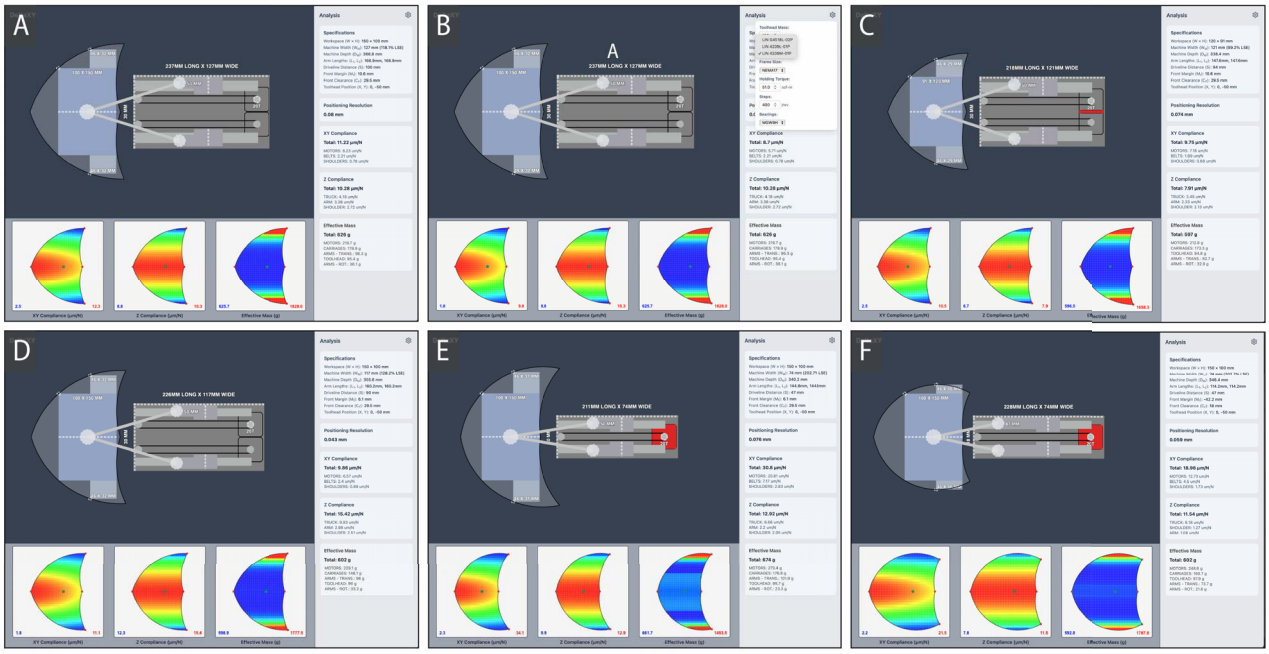

Figure 36: A hypothetical workflow to design a rackable solder paste dispenser, that includes A) setting the workspace to 150x100mm, B) selecting a smaller step-size motor, C) observing motor interference below a certain base width, D) changing to narrower bearing rails, E) intentionally overlapping both motors, F) adjusting linkage parameters to improve positioning resolution.

pre-programming. The latter approach could help the tool better fit into patterns of use established by existing benchtop equipment, where interactions are typically self-contained at the device rather than taking place at a computer.

9 Limitations and Future Work

9.1 Limitations of the DeltaXY Positioning Mechanism

Working Area. Working area is coupled to machine depth, and there is a practical limit to workspace dimensions beyond which the DeltaXY architecture no longer makes sense due to depth requirements (explored in Sec. 7.3). Additionally, traditional desktop digital fabrication tools become more spatially efficient at larger sizes due to relatively fixed mechanical overhead, reducing the benefit of DeltaXY. Based on our approximations of Fig. 27, DeltaXY is likely to be particularly useful for working areas of about 200mm and smaller, where overall machine depth remains under 600mm (24").

Stiffness and Positioning Resolution. DeltaXY's cantilevered toolhead is inherently less stiff vertically than architectures where a gantry is supported on both sides. This is addressable through appropriate design of the bearings and arms. The DeltaXY mechanism amplifies motion between its actuators and toolhead, putting it at a disadvantage in terms of lateral resolution and stiffness. We believe that suitable performance can be achieved for many applications through thoughtful mechanical design.

Non-Linearity. DeltaXY is non-linear in the X direction and is more sensitive to misalignment than traditional Cartesian machines, as we discuss in Sec. 4.5. We demonstrate that we were able to achieve good accuracy through simple calibration procedures.

9.2 Limitations of the LSE Metric

The metric of lateral spatial efficiency (LSE) becomes nuanced when a toolhead is able to transit laterally outside the static envelope of its parent machine. Figure 38 illustrates this situation for Fab Unit. The outer diameter $\varnothing_T$ of the toolhead occupies a total travel bounds W_E of 145mm (Fig. 38B) when its center traverses the full workspace width W of 120mm (Fig. 38A) as shown. We can state that $W_E = W + \varnothing_T$.

With a machine base width of 127mm, Fab Unit has an LSE of 94% according to our definition of $LSE = 120/127mm \left(\frac{W}{W_M}\right)$. There are situations where this metric remains valuable and meaningful. As described in Sec. 2.4, the toolhead always leads the arms when outside the lateral bounds of the machine base, which mostly limits the zone of potential interference to the cantilevered region of the workspace. When we situated Fab Unit in domestic and workshop settings as described in Sec. 5.1, we observed that adjacent objects were often at an elevation below that of the toolhead, and when not, we found it convenient to position Fab Unit so that the workbed overhung the shelf it was sitting on. This differs from e.g. bed slinger architectures (see Sec. 2.4), where the zone of interference both spans most of the machine width and is near the base of the device, making it difficult to avoid collisions. In situations like the

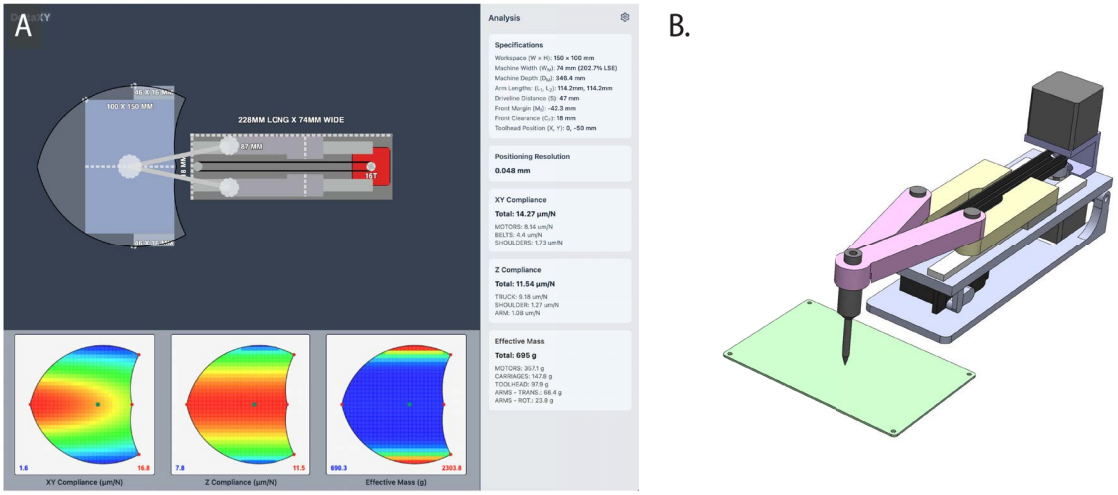

Figure 37: A preliminary design for an automated solder paste dispenser's positioning mechanism. A) The end result of the DeltaXY exploration process. B) A rough CAD model that was guided by the design tool output.

print farms described in Sec. 5.2, lateral toolhead excursion can limit the effective working area of simultaneously operating adjacent machines. However, it is possible to timeshare airspace, which can be naively accomplished by assigning jobs of compatible sizes to adjacent machines. Our sampling of the Thingiverse database (see Fig. 16) suggests that this may be a feasible approach for workspaces similar to Fab Unit's, because there is a high likelihood of any given print job not requiring the full workspace. This challenge might lead to future work on advanced scheduling algorithms that synchronize toolpaths dynamically across adjacent machines.

In certain contexts the LSE metric will overstate the effective lateral spatial efficiency of the machine. Print farm interactions may become more complicated if part assignment is required to avoid collisions. Machines that must be directly located against vertical surfaces like walls can suffer from reduced effective workspaces. To help users of rackable digital fabrication tools fully understand effective LSE for their situation, we propose an additional bounding metric of *minimum lateral spatial efficiency (MLSE)* that we define as the ratio of workspace width W to toolhead travel bounds W_E. MLSE is therefore limited by toolhead diameter $\varnothing_T$, such that

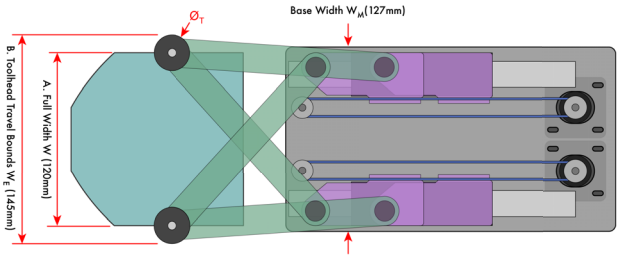

Figure 38: Fab Unit's Lateral Spatial Efficiency (LSE) and *Minimum LSE (MLSE)*

$MLSE = \left(\frac{W}{W+\varnothing_T}\right)$. Fab Unit has a basic toolhead diameter of 25mm, resulting in an MLSE of 82.7%. Referring to Fig. 4, we note that this remains significantly higher than commercial alternatives, which have LSEs of less than 50% for an equivalent build area width. During the course of this research we have experimented with mounting a fan on Fab Unit to improve print quality.

Our initial fan design increases the effective diameter of the toolhead to approximately 55mm, which decreases the MLSE to 68.5%. However, we are confident that subsequent development will result in a design that retains the original effective toolhead diameter of 25mm and an MLSE value of 82.7%.

9.3 Limitations of Analyses and Design Tool

We present a set of guidelines, analyses, and a browser-based design tool to aid researchers in utilizing DeltaXY. We have generally sought to decouple geometric properties such as resolution and compliance gain from estimates such as real-world actuator compliance and bearing stiffness. However, to illustrate how our design tool can assist in gaining an intuition for the design space of DeltaXY, we use real-world values based on these estimates. Future work will seek to validate these against experimental results. Additionally, when typical motor torque specifications are applied to the metrics of effective mass and acceleration gain, the resulting acceleration values far exceed usual limits imposed by slicing software. Further work is required to understand real-world limiting factors for acceleration beyond reflected inertia, including friction and drivetrain compliance. We recommend using the metrics provided by the design tool in a comparative manner (i.e. between two design candidates, or between a design candidate and reflected inertia as measured or estimated on a benchmark machine). Lastly, we note that the design tool currently supports modifying mechanism geometry, and offers limited component selection. Future work will expand the dimensionality of the design tool to include additional component

choices such as motors and linear bearings, and adjustments to the arm cross-sections that impact Z compliance values.

10 Conclusions

In this paper we present Cantilevered DeltaXY, a 2D positioning mechanism with an exceptionally high lateral spatial efficiency that opens the door to shelf-situated *rackable* digital fabrication tools as a new design space for HCI digital fabrication research. We enable this by contributing a reference mechanism for DeltaXY, a set of analytical and graphical design tools to aid in its adaptation to new lines of inquiry, and a working prototype of a bookshelf 3D printer that uncovers practical implementation considerations. We discuss the impact of rackable digital fabrication on where machines can be placed, how they might enable digital fabrication "farms" in contexts where they currently do not exist, and begin to outline a vision for sub-industrial digital fabrication factories. All of these have implications for how we might interact with digital fabrication tools, what they empower to be achieved, and by whom. We hope that this work, including our open-source design files and design software tools, will enable greater exploration and validation of rackable digital fabrication form-factors.

Acknowledgments

This research is based in part on work enabled by a gift from TTS Tooltechnic Systems and support from the David S.Y. (1962) and Patrick Wong Fellowship Fund. It was additionally funded in part by the National Institute of Standards and Technology, Grant Number 70NANB23H034-4, and the National Science Foundation, Grant Number 2441766. The authors gratefully acknowledge these sources of support. Any opinions, findings, and conclusions or recommendations expressed in this material are those of the authors and do not necessarily reflect the views of funding institutions. This work first took shape during Prof. Neil Gershenfeld's course "How to Make Something that Makes (almost) Anything" in the Spring of 2024. We are thankful for the support and encouragement of the teaching staff and our fellow students, as well as the wonderful and inspiring machine building community — including Jake Read and Nadya Peek — at the MIT Center for Bits and Atoms over the past two decades. Fabrication of Fab Unit was supported by the invaluable help of Mark Belanger at the MIT Edgerton Center Student Shop and Hayami Arakawa at the MIT Hobby Shop. The University of North Carolina at Chapel Hill's "Be A Maker" (BeAM) makerspaces also provided kind support to this project. We would like to thank Professor Alex Slocum for his inspiration and his insightful suggestions, and Aditya Ghodgaonkar and Alan Papalia for their thoughtful feedback. Lastly, we thank Alan Papalia and the students of MIT 2.S02 "Tool Design" (Spring 2024) for helping to stimulate this work.

References

[1] Paul P Acarnley. 2002. *Stepping motors: a guide to theory and practice.* Number 63. Iet.
[2] Andrew Allcock. 2003. In Search of One. *Machinery* (Nov. 21 2003).
[3] Michelle Annett, Tovi Grossman, Daniel Wigdor, and George Fitzmaurice. 2019. Exploring and understanding the role of workshop environments in personal fabrication processes. *ACM Transactions on Computer-Human Interaction (TOCHI)* 26, 2 (2019), 1–43.
[4] Prusa Research a.s. 2025. Original Prusa MK4S 3D Printer. https://www.prusa3d.com/product/original-prusa-mk4s-3d-printer-5/ Accessed on Aug. 27, 2025.
[5] Patrick Baudisch, Stefanie Mueller, et al. 2017. Personal fabrication. *Foundations and Trends® in Human–Computer Interaction* 10, 3–4 (2017), 165–293.
[6] BIGTREETECH. 2024. Manta-M4P GitHub Repository. https://github.com/bigtreetech/Manta-M4P. Accessed: September 13, 2024.
[7] Mohamed Bouri and Reymond Clavel. 2010. The linear delta: Developments and applications. In *ISR 2010 (41st International Symposium on Robotics) and ROBOTIK 2010 (6th German Conference on Robotics)*. VDE, IEEE, 1–8.
[8] Daniel Campos Zamora, Liang He, and Jon E Froehlich. 2024. MobiPrint: A Mobile 3D Printer for Environment-Scale Design and Fabrication. In *Proceedings of the 37th Annual ACM Symposium on User Interface Software and Technology*. Association for Computing Machinery, 1–10.
[9] ArcDroid CNC. 2025. ArcDroid CNC. https://arcdroidcnc.com Accessed on Aug. 28, 2025.
[10] Miguel De La Melena and Shawn Duan. 2024. New Design and Prototype of Two Degrees-of-Freedom Planar Parallel Manipulator for Use in Creating an Infinite 3D Printer. *Journal of Mechanisms and Robotics* 16, 9 (2024).
[11] Fluidd. 2026. Fluidd Documentation. https://docs.fluidd.xyz. https://docs.fluidd.xyz Accessed: February 6th, 2026.
[12] Frikk Fossdal, Rogardt Heldal, and Nadya Peek. 2021. Interactive digital fabrication machine control directly within a CAD environment. In *Proceedings of the 6th Annual ACM Symposium on Computational Fabrication*. Association for Computing Machinery, 1–15.
[13] Frikk H Fossdal, Jens Dyvik, Jakob Anders Nilsson, Jon Nordby, Torbjørn Nordvik Helgesen, Rogardt Heldal, and Nadya Peek. 2020. Fabricatable machines: A toolkit for building digital fabrication machines. In *Proceedings of the fourteenth international conference on tangible, embedded, and embodied interaction*. Association for Computing Machinery, 411–422.
[14] Frikk H Fossdal, Vinh Nguyen, Rogardt Heldal, Corie L Cobb, and Nadya Peek. 2023. Vespidae: A programming framework for developing digital fabrication workflows. In *Proceedings of the 2023 ACM Designing Interactive Systems Conference*. Association for Computing Machinery, 2034–2049.
[15] Neil Gershenfeld. 2012. How to make almost anything: The digital fabrication revolution. *Foreign Aff.* 91 (2012), 43.
[16] Neil A Gershenfeld. 2005. *Fab: the coming revolution on your desktop–from personal computers to personal fabrication.* Basic Books (AZ).
[17] Dr. Fritz Faulhauber GmbH. 2020. *Stepper Motor Technical Note: Microstepping Myths and Realities.* Technical Report.
[18] Jamison Go and A John Hart. 2017. Fast desktop-scale extrusion additive manufacturing. *Additive Manufacturing* 18 (2017), 276–284.
[19] Michael Goldberg. 1942. Polyhedral linkages. *National Mathematics Magazine* 16, 7 (1942), 323–332.
[20] Clement Gosselin, Jorge Angeles, et al. 1990. Singularity analysis of closed-loop kinematic chains. *IEEE transactions on robotics and automation* 6, 3 (1990), 281–290.
[21] Ivan Grgić, Mirko Karakašić, Hrvoje Glavaš, and Pejo Konjatić. 2023. Accuracy of FDM PLA polymer 3D printing technology based on tolerance fields. *Processes* 11, 10 (2023), 2810.
[22] Georg Hanrath and Gerald Stengele. 2001. Machine Tool for Triaxial Machining of Work Pieces. https://patents.google.com/patent/US6328510 US Patent 6,328,510.
[23] Shiqing He and Eytan Adar. 2020. Plotting with thread: Fabricating delicate punch needle embroidery with xy plotters. In *Proceedings of the 2020 ACM designing interactive systems conference*. Association for Computing Machinery, 1047–1057.
[24] Nathaniel Hudson, Celena Alcock, and Parmit K Chilana. 2016. Understanding newcomers to 3D printing: Motivations, workflows, and barriers of casual makers. In *Proceedings of the 2016 CHI conference on human factors in computing systems*. Association for Computing Machinery, 384–396.
[25] Alexander Htet Kyaw, Miana Smith, Se Hwan Jeon, and Neil Gershenfeld. 2025. Speech to Reality: On-Demand Production using Natural Language, 3D Generative AI, and Discrete Robotic Assembly. In *Proceedings of the ACM Symposium on Computational Fabrication*. Association for Computing Machinery, 1–12.
[26] Bambu Lab. 2025. Bambu Lab A1 mini. https://bambulab.com/en-us/a1-mini Accessed on Aug. 27, 2025.
[27] Will Langford and Sam Calisch. 2012. Foldafab. https://mtm.cba.mit.edu/2012/2012_foldafab/deploy/index.html. Accessed: September 12, 2025.
[28] Chun-Ying Lee and Chung-Yin Liu. 2019. The influence of forced-air cooling on a 3D printed PLA part manufactured by fused filament fabrication. *Additive Manufacturing* 25 (2019), 196–203.
[29] Jessica Lingel. 2016. The poetics of socio-technical space: Evaluating the internet of things through craft. In *Proceedings of the 2016 CHI Conference on Human Factors in Computing Systems*. Association for Computing Machinery, 815–826.
[30] Fangzheng Liu and Joseph A Paradiso. 2023. Printedcircuit board (pcb) probe tester (pcbpt)-a compact desktop systemthat helps with automatic pcbdebugging. In *Adjunct Proceedings of the 36th Annual ACM Symposium on User Interface Software and Technology*. Association for Computing Machinery, 1–3.
[31] Xin-Jun Liu, Qi-Ming Wang, and Jinsong Wang. 2005. Kinematics, dynamics and dimensional synthesis of a novel 2-DoF translational manipulator. *Journal of Intelligent and Robotic Systems* 41 (2005), 205–224.

[32] Hiroshi Makino. 2014. Development of the SCARA. *Journal of Robotics and Mechatronics* 26, 1 (2014), 5–8.

[33] John Mazurkiewicz. 1995. The basics of motion control—Part 1. *Power Transmission Design* (1995), 43–45.

[34] D McCloy. 1990. Some comparisons of serial-driven and parallel-driven manipulators. *Robotica* 8, 4 (1990), 355–362.

[35] Christian McKay and Kylie Peppler. 2013. MakerCart: A mobile fab lab for the classroom. In *Position Paper at the Interaction Design for Children Conference (IDC)*. Association for Computing Machinery.

[36] J-P Merlet. 2006. *Parallel Robots*. Springer.

[37] Ilan Moyer. 2012. CoreXY. https://www.corexy.com/index.html Accessed on Aug. 28, 2025.

[38] Ilan Ellison Moyer. 2013. *A gestalt framework for virtual machine control of automated tools*. Ph. D. Dissertation. Massachusetts Institute of Technology.

[39] Ilan E Moyer, Samuelle Bourgault, Devon Frost, and Jennifer Jacobs. 2024. Throwing Out Conventions: Reimagining Craft-Centered CNC Tool Design through the Digital Pottery Wheel. In *Proceedings of the 2024 CHI Conference on Human Factors in Computing Systems* (Honolulu, HI, USA) *(CHI '24)*. Association for Computing Machinery, New York, NY, USA, Article 347, 22 pages. https://doi.org/10.1145/3613904.3642361

[40] Daniel Norée. 2020. 3DBenchy - The jolly 3D printing torture-test. https://www.3dbenchy.com Accessed on Feb. 4, 2026.

[41] Kevin O'Connor. 2026. Klipper 3D Printer Firmware. https://www.klipper3d.org/. https://www.klipper3d.org/ Accessed: February 6, 2026.

[42] Zoran Pandilov and Vladimir Dukovski. 2012. Parallel kinematics machine tools: Overview-from history to the future. *Annals of the Faculty of Engineering Hunedoara* 10, 2 (2012), 111.

[43] PavloG on RepRap.org. 2016. DeltaXY. https://reprap.org/forum/read.php?178,666239. Accessed: December 10, 2024.

[44] Nadya Peek, James Coleman, Ilan Moyer, and Neil Gershenfeld. 2017. Cardboard machine kit: Modules for the rapid prototyping of rapid prototyping machines. In *Proceedings of the 2017 CHI Conference on Human Factors in Computing Systems*. Association for Computing Machinery, 3657–3668.

[45] Nadya Peek and Ilan Moyer. 2017. Popfab: A case for portable digital fabrication. In *Proceedings of the Eleventh International Conference on Tangible, Embedded, and Embodied Interaction*. Association for Computing Machinery, 325–329.

[46] Nadya Nadya Meile Peek. 2016. *Making machines that make: object-oriented hardware meets object-oriented software*. Ph. D. Dissertation. Massachusetts Institute of Technology.

[47] Raimund Perneder and Ian Osborne. 2012. *Handbook timing belts: principles, calculations, applications*. Springer Science & Business Media.

[48] 3D Potter. 2025. 3D Potterbot SCARA v4. https://3dpotter.com/product/3d-potterbot-scara-v4/ Accessed on Aug. 28, 2025.

[49] Cocoa Press. 2025. Cocoa Press 3D Chocolate Printer. https://cocoapress.com Accessed on Dec. 4, 2025.

[50] Hao Qi, Guan Liwen, and Wang Jianxin. 2012. Dynamic performance evaluation of a 2-DoF planar parallel mechanism. *International journal of advanced robotic systems* 9, 6 (2012), 250.

[51] Jake Robert Read, Leo McElroy, Quentin Bolsee, B Smith, and Neil Gershenfeld. 2023. Modular-things: plug-and-play with virtualized hardware. In *Extended abstracts of the 2023 CHI conference on human factors in computing systems*. Association for Computing Machinery, 1–6.

[52] Jake Robert Read, Nadya Peek, and Neil Gershenfeld. 2023. Maxl: distributed trajectories for modular motion. In *Proceedings of the 8th ACM Symposium on Computational Fabrication*. Association for Computing Machinery, 1–11.

[53] Michael L Rivera and Scott E Hudson. 2019. Desktop electrospinning: a single extruder 3D printer for producing rigid plastic and electrospun textiles. In *Proceedings of the 2019 CHI Conference on Human Factors in Computing Systems*. Association for Computing Machinery, 1–12.

[54] Alec Rivers, Ilan E. Moyer, and Frédo Durand. 2012. Position-correcting tools for 2D digital fabrication. *ACM Trans. Graph.* 31, 4, Article 88 (July 2012), 7 pages. https://doi.org/10.1145/2185520.2185584

[55] Rob Stuart. 2017. Deltesian. https://bornity.com/deltesian. Accessed: Aug. 28, 2025.

[56] Carolyn Schwaar. 2024. A 3D Printer On Every Desk? Why Companies Are Buying More 3D Printers. *Forbes* (2024). https://www.forbes.com/sites/carolynschwaar/2024/05/02/a-3d-printer-on-every-desk-why-companies-are-buying-more-3d-printers/

[57] Inc. Shaper Tools. 2025. Shaper Origin Handheld CNC Router. https://www.shapertools.com/en-us/origin Accessed on Dec. 3, 2025.

[58] Rita Shewbridge, Amy Hurst, and Shaun K Kane. 2014. Everyday making: identifying future uses for 3D printing in the home. In *Proceedings of the 2014 conference on Designing interactive systems*. Association for Computing Machinery, 815–824.

[59] Alexander Slocum. 2008. FUNdaMENTALS of Design.

[60] Alexander H Slocum. 1992. *Precision machine design*. Society of Manufacturing Engineers.

[61] Seungkil Son, Taejung Kim, Sanjay E Sarma, and Alexander Slocum. 2009. A hybrid 5-axis CNC milling machine. *Precision Engineering* 33, 4 (2009), 430–446.

[62] Evgeny Stemasov, Enrico Rukzio, and Jan Gugenheimer. 2021. The road to ubiquitous personal fabrication: Modeling-free instead of increasingly simple. *IEEE Pervasive Computing* 20, 1 (2021), 19–27.

[63] Blair Subbaraman, Orlando de Lange, Sam Ferguson, and Nadya Peek. 2024. The Duckbot: A system for automated imaging and manipulation of duckweed. *Plos one* 19, 1 (2024), e0296717.

[64] Blair Subbaraman and Nadya Peek. 2022. p5. fab: direct control of digital fabrication machines from a creative coding environment. In *Proceedings of the 2022 ACM Designing Interactive Systems Conference*. Association for Computing Machinery, 1148–1161.

[65] Blair Subbaraman and Nadya Peek. 2024. Playing the Print: MIDI-Based Fabrication Interfaces to Explore and Document Material Behavior. In *Extended Abstracts of the CHI Conference on Human Factors in Computing Systems*. Association for Computing Machinery, 1–8.

[66] Haruki Takahashi and Kohei Matsumura. 2025. Press the Button to 3D Print: Lowering Barriers to 3D Printing with a Single-Button Interface. In *Proceedings of the ACM Symposium on Computational Fabrication*. Association for Computing Machinery, 1–13.

[67] Rundong Tian, Vedant Saran, Mareike Kritzler, Florian Michahelles, and Eric Paulos. 2019. Turn-by-wire: Computationally mediated physical fabrication. In *Proceedings of the 32nd annual ACM symposium on user interface software and technology*. Association for Computing Machinery, 713–725.

[68] Bantam Tools. 2025. Bantam Tools NextDraw 8511. https://bantamtools.com/products/bantam-tools-nextdraw-8511 Accessed on Dec. 3, 2025.

[69] Jasper Tran O'Leary, Gabrielle Benabdallah, and Nadya Peek. 2023. Imprimer: Computational Notebooks for CNC Milling. In *Proceedings of the 2023 CHI conference on human factors in computing systems*. Association for Computing Machinery, 1–15.

[70] Jasper Tran O'Leary, Thrisha Ramesh, Octi Zhang, and Nadya Peek. 2024. Tandem: Reproducible Digital Fabrication Workflows as Multimodal Programs. In *Proceedings of the 2024 CHI Conference on Human Factors in Computing Systems*. Association for Computing Machinery, 1–16.

[71] UltiMaker. 2025. Shop UltiMaker S3 3D Printer. https://store.ultimaker.com/3d-printers/s-series/ultimaker-s3-3d-printer Accessed on Dec. 4, 2025.

[72] Joshua Vasquez, Hannah Twigg-Smith, Jasper Tran O'Leary, and Nadya Peek. 2020. Jubilee: An extensible machine for multi-tool fabrication. In *Proceedings of the 2020 CHI Conference on Human Factors in Computing Systems*. Association for Computing Machinery, 1–13.

[73] Karl DD Willis, Cheng Xu, Kuan-Ju Wu, Golan Levin, and Mark D Gross. 2010. Interactive fabrication: new interfaces for digital fabrication. In *Proceedings of the fifth international conference on Tangible, embedded, and embodied interaction*. Association for Computing Machinery, 69–72.

[74] Jun Wu, Dong Wang, and Liping Wang. 2015. A control strategy of a two degrees-of-freedom heavy duty parallel manipulator. *Journal of Dynamic Systems, Measurement, and Control* 137, 6 (2015).

[75] Shanjiang Zhang and Guanglu Liu. 2024. Design of a multipurpose SCARA-like parallel robot. In *2024 4th International Symposium on Artificial Intelligence and Intelligent Manufacturing (AIIM)*. IEEE, 18–21.

[76] Amit Zoran and Marcelo Coelho. 2011. Cornucopia: the concept of digital gastronomy. *Leonardo* 44, 5 (2011), 425–431.

[77] Amit Zoran and Joseph A Paradiso. 2013. FreeD: a freehand digital sculpting tool. In *Proceedings of the SIGCHI conference on human factors in computing systems*. Association for Computing Machinery, 2613–2616.

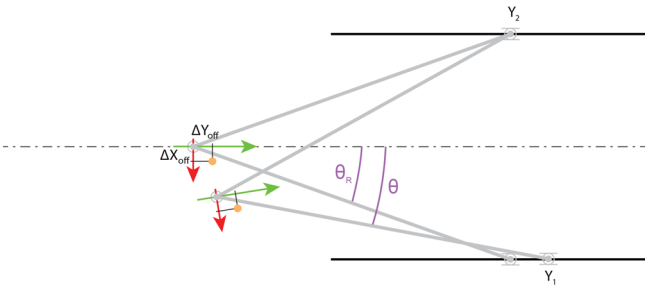

Figure 39: Modeling of an offset of the toolhead relative to the pivot. In this example, the toolhead is attached on the lower arm, and rotates with it. The toolhead's offsets ΔX_{off}, ΔY_{off} are provided in the local coordinate system rotating with the arm.

A Kinematics of an Off-Center Toolhead

When the toolhead is not centered on the pivot, the offset needs to be taken into account in the kinematic model. Figure 39 illustrates the offset vector $(\Delta X_{\text{off}},\ \Delta Y_{\text{off}})$ in the local coordinate system of the toolhead. This coordinate system is only aligned with the global coordinate system when the machine is at rest, that is: $Y_1 = Y_2$.

In this example, the toolhead is attached to the arm at the bottom of the figure. To derive the inverse kinematic equations, let us first define the angle *theta* between this arm and the centerline, given the difference $A' = Y_1 - Y_2$:

$$\theta = \frac{\pi}{2} - \tan^{-1}\left(\frac{A'}{S}\right) - \cos^{-1}\left(\frac{\sqrt{A'^2 + S^2}}{2L}\right) \tag{21}$$

At rest, $A' = 0$ and the angle simplifies to:

$$\theta_R = \frac{\pi}{2} - \cos^{-1}\left(\frac{S}{2L}\right) \tag{22}$$

The difference in angle $\Delta\theta = \theta - \theta_R$ provides the amount of rotation applied on the local coordinate system of the toolhead. The local X-axis is the vector $(\cos(\Delta\theta),\ \sin(\Delta\theta))$, while the local Y-axis is $(-\sin(\Delta\theta),\ \cos(\Delta\theta))$. In conjunction with the offset parameters $(\Delta X_{\text{off}},\ \Delta Y_{\text{off}})$, the toolhead position provided by Equations 9 and 10 can be corrected:

$$X'_T = X_T + \cos(\Delta\theta)\Delta X_{\text{off}} - \sin(\Delta\theta)\Delta Y_{\text{off}} \tag{23}$$

$$Y'_T = Y_T + \sin(\Delta\theta)\Delta X_{\text{off}} + \cos(\Delta\theta)\Delta Y_{\text{off}} \tag{24}$$